REGULATION OF PEAMT ACTIVITY IN SPINACH

REGULATION OF *S*-ADENOSYL-L-METHIONINE: PHOSPHOETHANOLAMINE-*N*-METHYLTRANSFERASE ACTIVITY IN SPINACH

By

MARTINA DREBENSTEDT, B.Sc.

A Thesis

Submitted to the School of Graduate Studies

in Partial Fulfilment of the Requirements

for the Degree

Master of Science

McMaster University

MASTER OF SCIENCE (2001)
(Biology)

McMaster University
Hamilton, Ontario

TITLE: Regulation of *S*-adenosyl-L-methionine phosphoethanolamine-*N*-methyltransferase Activity in Spinach

AUTHOR: Martina Drebenstedt, B.Sc. (McMaster University)

SUPERVISOR: Dr. Elizabeth Weretilnyk

NUMBER OF PAGES: xii, 114

ABSTRACT

The compatible solute glycine betaine accumulates in many plants including spinach (*Spinacea oleracea*) under conditions of water deficit stress. The precursor to glycine betaine is choline, a ubiquitous metabolite in plants as a component of phosphotidylcholine. In spinach choline is synthesized from phosphocholine, a product of three sequential *N*-methylations of phosphoethanolamine catalysed by the cytosolic enzyme *S*-adenosyl-L-methionine: phosphoethanolamine-*N*-methyltransferase (PEAMT). PEAMT activity shows diurnal changes with peak activity at the end of the photoperiod and a decrease overnight. The activity of this enzyme is up-regulated 2 to 3-fold in salt-stressed plants relative to unstressed plants. The objective of this thesis is to determine how PEAMT activity is regulated *in vivo*. Thus, PEAMT activity, protein and transcript levels were quantified in spinach leaves from plants subjected to different light and salinity conditions.

A spinach PEAMT cDNA sequence was used to over-express recombinant PEAMT in the protein expression vector pET30a (+). The presence of a polyhistidine-tag on the overexpressed protein allowed for purification by a cobalt metal affinity column. The affinity purified protein was used to produce polyclonal antibodies for immunoblot hybridization analysis. For these studies, PEAMT protein was first immunoaffinity purified from soluble extracts prepared from leaves and then the protein subjected to electrophoresis by SDS-PAGE. Enzyme assays and immunoblot analysis show PEAMT activity and protein levels

increase and become relatively constant in leaves of plants exposed to continuous light. In continuous darkness, PEAMT activity and protein levels decrease and remain low and constant. Thus the pattern of changes in PEAMT activity levels are associated with changes in PEAMT protein levels. In contrast, Northern blot hybridizations show that under conditions of constant light, *peamt* transcript levels undergo cyclical changes with peak levels at 20 and 40 h and troughs at 28 and 52 h after the continuous light treatment was imposed. These peaks coincide with the dark and light cycles of the normal photoperiod. The same cyclical changes in *peamt* transcript levels was seen for plants transferred from a normal photoperiod to continuous darkness. Since these changes persist in the absence of a day/night cue we conclude that *peamt* transcript levels are circadian-regulated. The *peamt* transcript levels of control unstressed and salt-stressed plants also show circadian rhythms, however the levels found in salt-stressed plants were 0.5 to 2-fold higher than the controls. Therefore, while salinization of plants increases *peamt* transcript abundance, it does not alter the circadian rhythm that transcripts of this gene display. Changes in PEAMT activity and protein levels are likely controlled by other as yet unknown post-translational mechanisms, processes that override and obscure operation of a circadian rhythm in regulating the level of *peamt* transcripts.

ACKNOWLEDGEMENTS

I would like to express my appreciation for the assistance and support given by so many. Sincere thanks must first go to my supervisor Dr. Elizabeth Weretilnyk for teaching me laboratory, computer and writing skills and Dr. Peter Summers who was indispensable in the lab and helped whenever I was having problems with anything. I would also like to thank my committee members Dr. George Sorger and Dr. John Lott for their help in making sure my thesis was on track. Thank you Dad and Ma for all your understanding and patience over the last two years. To my good friends Holly, Amy, Tom and Corinne, thanks for all your help and support.

TABLE OF CONTENTS

LIST OF FIGURES

APPENDICES

LIST OF ABBREVIATIONS

ADK	Adenosine kinase
ATP	Adenosine triphosphate
BADH	Betaine aldehyde dehydrogenase
BSA	Bovine serum albumin
bp	Base pairs
cDNA	Complementary deoxyribonucleic acid
CDP-Cho	Cytidine diphosphate choline
CDP-DEA	Cytidine diphosphate dimethylethanolamine
CDP-EA	Cytidine diphosphate ethanolamine
CDP-MEA	Cytidine diphosphate methylethanolamine
CMO	Choline monooxygenase
cpm	Counts per minute
Cho	Choline
DEA	Dimethylethanolamine
DMSP	3-Dimethylsulfoniopropionate
DTT	Dithiothreitol
EDTA	Ethylenediaminetetraacetic acid
EA	Ethanolamine
HEPES	*N*-[2-hydroxyethyl]piperazine-*N*'-[2-ethanesulfonic acid]
IPTG	Isopropyl-β-D-thiogalactopyranoside
kbp	Kilobase pairs
kDa	Kilodaltons
LSU	Large subunit
MEA	Methylethanolamine

Mr	Molecular mass (relative)
OD	Optical density
P-base	Phospho-base
PCho	Phosphocholine
PDEA	Phosphodimethylethanolamine
PDEAMT	Phosphodimethylethanolamine-*N*-methyltransferase
PEA	Phosphoethanolamine
PEAMT	*S*-adenosyl-L-methionine phosphoethanolamine-*N*-methyltransferase
PMEA	Phosphomethylethanolamine
PMEAMT	Phosphomethylethanolamine-*N*-methyltransferase
Ptd	prefix Phosphatidyl
PtdCho	Phosphatidylcholine
PtdDEA	Phosphatidyldimethylethanolamine
PtdEA	Phosphatidylethanolamine
PtdMEA	Phosphatidylmethylethanolamine
QAC	Quaternary ammonium compound
Rubisco	Ribulose-1,5-bisphosphate carboxylase-oxygenase
SAH	*S*-adenosyl-L-homocysteine
SAHH	*S*-adenosyl-L-homocysteine hydrolase
SAM	*S*-adenosyl-L-methionine
SDS	Sodium dodecyl sulphate
SDS-PAGE	Sodium dodecyl sulphate-polyacrylamide gel electrophoresis
Tris	Tris(hydroxymethyl)aminomethane
UV	Ultraviolet

LITERATURE REVIEW

Plants show highest productivity in their physiologically and ecologically optimal environments, but natural conditions are rarely optimal (Epstein and Rains, 1987) . Plants must survive a wide array of environmental factors that may impact upon their productivity. An environmental condition that exerts an unfavourable or injurious strain on a plant is a stress (Rhodes, 1987). Some of the principal environmental stresses affecting plants include high or low temperature, excess or deficit of water, salinity, light quality, chemical and biotic interactions (Rhodes, 1987).

A wide range of metabolic responses can be induced by stress (Hanson and Hitz, 1982). Many of these responses are adaptive and involve readjusting metabolism to a steady state through stress avoidance or tolerance and allowing the continuation of growth after the stress is relieved (Koshland, 1984). However, some changes in a plant caused by environmental factors are not adaptive and have either no impact or a deleterious effect on survival (Hanson and Hitz, 1982). The mechanisms mediating the response can involve a variety of changes in the plant such as altered gene expression, cellular metabolism and growth rate (Bray *et al.*, 2000). The ways in which plants respond to stress are important both to agriculture and ecology (Boyer, 1982; Taiz and Zeiger, 1998). Environmental stresses can influence crop yield and when productivity is reduced crop losses in excess of

50% are possible (Boyer, 1982). Moreover, in natural ecosystems the ecological distribution of land plants is influenced greatly by the stresses encountered in any environment (Kramer, 1983).

Land plants are more affected by the availability of water than any other factor required by plants for growth (Kramer, 1983). Water is a necessary constituent of plants making up as much as 90% of leaf fresh weight in some plants (Raven *et al.*, 1999). Water is the medium in which nutrients pass in and out of the cell, water is required as a substrate in many plant metabolic processes and water maintains plant turgidity (Bewley, 1979). Lack of water is considered to be the most serious environmental stress (Boyer, 1982). Both drought and saline conditions can lead to a water deficit in plants (Rhodes, 1987).

Water Relations

Water movement in plants has been described in terms of gradients of water potential (Ψ_w), a term which is expressed in units of pressure (Kramer 1983). Ψ_w decreases in solutions as the solute concentration increases; in the absence of any solutes Ψ_w is zero such that the presence of solutes invariably makes Ψ_w a negative value. The water stress of a plant cell increases as the Ψ_w becomes more negative, thus a measurement of Ψ_w of a plant organ or cell can be used to estimate the degree of hydration in part of or the entire plant (Bray *et al.*, 2000). Ψ_w is made up of several component potentials in the following relationship:

$$\Psi_w = \Psi_s + \Psi_p + \Psi_g + \Psi_m$$

Solute potential (Ψ_s) describes the amount of dissolved particles in water. The pressure

potential (Ψ_p) shows the effect of the physical forces in the environment on Ψ_w. Negative pressure or tension decreases Ψ_w and positive pressure as turgor increases Ψ_w. Gravitational potential (Ψ_g) is the downward pull of water by gravity which has a minimal effect on water movement between cells or even between various organs in small plants. Gravitational potential is therefore usually omitted from the equation. Matric potential (Ψ_m) is the interaction of water with solid surfaces usually in thin layers which can depress water potential. However, as matric potential is very small and difficult to measure it is also generally omitted from the equation for water potential. Thus a simplified water potential equation can be used:

$$\Psi_w = \Psi_s + \Psi_p \qquad \text{(Bray } et\ al.\text{, 2000).}$$

Water potential is useful in evaluating the water status or degree of hydration of the plant (Taiz and Zeiger, 1998). Water moves across plant cell membranes along water potential gradients with movement in the direction from high to lower Ψ_w. When cells lose water, solutes remaining behind are passively concentrated (Taiz and Zeiger, 1998). When flaccid, cells have an internal pressure equal to ambient pressure (0 MPa) and a high solute concentration, hence low solute potential with both factors contributing to a low Ψ_w. When the cell is in an environment with a higher water potential, water will move into the cell along a gradient of Ψ_w. If available water flows into the cell, volume increases and the pressure potential or turgor will rise as the cell walls resist enlargement. This increase in turgor and dilution of cellular solutes raises the Ψ_w of the cell to the same Ψ_w value as the surrounding

environment (Taiz and Zeiger, 1998). At this point an equilibrium can be established and the net inward flow of water would stop. Conversely, water moves out of the cell when it is in a medium with a lower Ψ_w. Thus gradients of water potential define how water moves across membranes and between cells in a plant (Bray *et al.*, 2000).

The leaves of well watered plants tend to have high solute potentials whereas those of halophytes can be very low (Morgan, 1986). Halophytes are species that tolerate and even thrive in high soil salinity. In contrast, plants that cannot complete their life cycle in saline environments are glycophytes. There is, however, a group of glycophytes found in non-saline environments that can develop the capacity to tolerate saline conditions (Hasegawa *et al.*, 2000).

The soil Ψ_w the plant experiences is one factor determining root Ψ_w. The plant absorbs water through its root hairs and the driving force for water absorption is the transpirational pull of water by water loss from leaves and a gradient of Ψ_w created by low xylem Ψ_w caused by high solute concentrations in the xylem sap of roots (Kramer, 1983). Water moves through the soil by bulk flow along a pressure gradient. As the roots absorb water from soil, the pressure potential of the water near the root decreases relative to water outside the root zone thereby establishing a pressure gradient such that water moves continuously into the root zone through spaces in the soil (Taiz and Zeiger, 1998). In well watered-soils soil water solute concentration is usually low and so soil Ψ_s approaches 0. However, saline soils can have very high solute concentrations leading to low soil Ψ_s making

extraction of water from the soil by the roots more difficult (Bray *et al.*, 2000).

The initial responses to declining soil water are stomatal closure and reduced plant growth rate (Davies *et al.*, 1990). Stomatal closure causes gas exchange to slow and thus transpiration and photosynthesis are effected (Davies *et al.*, 1990; Yeo *et al.*, 1985). Nutritional imbalances are caused by direct toxicity of accumulated ions in the tissues (Apse *et al.*, 1999; Hasegawa *et al.*, 2000). Moreover, there are large energy costs associated with surviving saline environments (McCree, 1986). Energy is expended for osmotic regulation as opposed to growth and for ion transport and storage (McCree, 1986). These adverse affects are due, in part, to the mechanisms of protection against salinity. Plant responses that protect against tissue water loss occur through stomatal closure, increased cuticle thickness, fewer stomata per leaf area, and increased root/shoot ratio (Pasternak, 1987). Increased water uptake is made possible through osmotic adjustment, a process whereby plants change their solute potential to maintain a positive turgor pressure (Bray *et al.*, 2000).

Osmotic Adjustment

As described above, Ψ_w is the sum of Ψ_s and Ψ_p. Therefore, when a plant experiences water deficit and Ψ_w decreases, an increase in the concentration of solutes can provide a driving force for water uptake in order to maintain a positive Ψ_p and prevent turgor loss. Osmotic adjustment in plant cells is the process whereby solutes are accumulated with the outcome of lower Ψ_s and hence root Ψ_w relative to soil Ψ_w thereby allowing water movement into the plant from the soil (Nilsen and Orcutt, 1996). Solute accumulation is seen

as an adaptive response to water deficit and is both a tolerance and avoidance mechanism (Storey and Wyn Jones, 1977; Rhodes, 1987). Saline conditions and drought as well as cold temperatures can elicit this response in plants (Nilsen and Orcutt, 1996). A variety of solutes are used by cells for osmotic adjustment depending on the availability of nutrients and species differences in osmotic adjustment strategies (Wyn Jones and Gorham, 1983). Accumulating inorganic ions such as potassium (K^+), calcium (Ca^{2+}) and sodium (Na^+) is considered energetically inexpensive as they only require transport to the vacuole (Nilsen and Orcutt, 1996). However, these ions are toxic to the cytoplasm when present in high concentrations since their accumulation could cause potential problems through interactions with proteins and other cellular components (Rhodes, 1987; Nilsen and Orcutt, 1996). Ion toxicity is avoided by accumulating osmotically active compounds that are non-toxic including those that can protect enzymes and membranes. These organic solutes are termed compatible solutes (Bray *et al.*, 2000). Compatible solutes exhibiting protective functions are called **osmoprotectants** (Bray *et al.*, 2000). Other means of avoiding ion toxicity include selective uptake of ions into cells through gated channels and the transport and compartmentalization of ions (Yeo, 1998). Thus while for many halophytic species the inorganic ions Na^+ and Cl^- generate most of the tissue pressure potential (Wyn Jones and Gorham, 1977; Jolivet *et al.*, 1983), another group of organic compatible solutes must be accumulated by halophytic and glycophytic plants that are non-toxic or non-perturbing to plant metabolism even at high concentrations (Bray *et al.*, 2000).

Compatible solutes

Compatible solutes used in osmotic adjustment share features in that they tend to be excluded from protein surfaces and their immediate hydration sphere, they are highly soluble, neutrally charged, and stable at physiological pH (Rhodes, 1987; McCue and Hanson, 1990; Bray *et al.*, 2000). Some compatible solutes accumulated by plants include amino acids, onium compounds and polyols/sugars. The amino acid proline is known to accumulate rapidly in water deficit stressed plants and is catabolized when the stress is alleviated making osmotic adjustment involving proline a reversible process (Bray *et al.*, 2000). Two types of onium compounds are quaternary ammonium compounds (QAC) and tertiary sulfonium compounds (TSC) (Nuccio *et al.*, 1999). The QAC glycine betaine is widespread among plant species (Storey and Wyn Jones, 1977) and is found in many families including the Asteraceae, Chenopodiaceae and Poaceae (Wyn Jones and Storey, 1981). Other QACs include proline betaine found in the Fabaceae and Lamiaceae and β-alanine betaine found in Plumbaginaceae (McCue and Hanson, 1990). TSCs include *β*-dimethylsulfoniopropionate (DMSP) found in Gramineae (McNeil *et al.*, 1999) and choline-*O*-sulfate found in Plumbaginaceae (McCue and Hanson, 1990;Hanson *et al.*, 1991; Rhodes and Hanson, 1993). Examples of polyols and sugars are mannitol, D-ononitiol and trehalose. The synthesis of these carbon based compatible organic compounds is relatively expensive for the plant as they require both carbon skeletons and ATP (Nilsen and Orcutt, 1996).

Glycine Betaine

Glycine betaine (*N,N,N*-trimethylglycine) is a QAC and is the simplest member of a group of *N*-methyl substituted amino acids (Wyn Jones and Storey, 1981). Glycine betaine was initially thought to be a metabolic waste product or perhaps have a role as a methyl donor. Storey and Wyn Jones (1975) were first to show a relationship in a number of plant species between glycine betaine accumulation and salt tolerance. Since then, the hypothesis that glycine betaine is a compatible solute important to cellular osmoregulation during salt stress has been supported through several lines of evidence (Storey and Wyn Jones, 1977; Grumet and Hanson, 1986). A survey of glycine betaine accumulating species shows that this QAC is accumulated to high levels by several species of halophytic, xerophytic and salt resistant glycophytic plants (Hanson and Scott, 1980; Wyn Jones and Storey, 1981; Rhodes and Hanson, 1993). Levels of glycine betaine increase in these species when plants are under conditions of water deficit stress (McDonnell and Wyn Jones, 1988; Müller and Eckert, 1989). Since the accumulation of glycine betaine coincides with decreasing Ψ_s in plant cells (Grumet and Hanson, 1986), elevated glycine betaine levels are believed to underlie changes in Ψ_s and so have an adaptive value for plants growing under conditions of low water availability (Guy *et al.*, 1984; Bray *et al.*, 2000).

As a non-toxic, neutral and stable compound, glycine betaine satisfies the properties of a compatible solute. Moreover, glycine betaine is localized in the cytoplasm and chloroplast of plant cells and is excluded from vacuoles; a subcellular distribution needed for osmotic regulation in the cytosol of cells containing vacuoles with osmotically active and potentially

toxic inorganic ions (Robinson and Jones, 1986). This QAC is normally found in higher concentrations in the shoot rather than root tissues of mature plants and while leaf tissue has been shown to synthesize glycine betaine *de novo*, roots have not (Wyn Jones and Storey, 1981; Grumet and Hanson, 1986). Glycine betaine is not broken down by plants (Bray *et al.*, 2000) and it is highly phloem mobile (McDonnell and Wyn Jones, 1988). Thus while high in young leaves, during growth glycine betaine can be reallocated to other parts of the plants resulting in the lower levels found in fully expanded leaves (Wyn Jones and Storey, 1981; Hanson and Wyse,1982; McDonnell and Wyn Jones, 1988). Since glycine betaine is not catabolized, it can accumulate during water deficit stress and persist in the plant to maintain tolerance. Following recovery of the plant from water stress the glycine betaine levels decrease in tissues as it is re-distributed to new tissue by translocation (Bray *et al.*, 2000).

Glycine Betaine Synthesis

In vivo radiotracer evidence shows that plants synthesize glycine betaine from choline by a two-step oxidation reaction with betaine aldehyde as the intermediate (Fig.1; Hanson *et al.*, 1985).

Choline monooxygenase (CMO)

The first oxidation step in the synthesis of glycine betaine is catalysed by CMO (Fig.1; Brouquisse *et al.*, 1989; Burnet *et al.*, 1995). CMO is a dimer of identical subunits with a molecular mass of 45 kD (Burnet *et al.*, 1995). This stromal enzyme shows light-induced activity with 10-fold lower activity detected in the dark (Weigel *et al.*, 1988). CMO

FIGURE 1: Glycine betaine synthesis

In the cytosol there are four theoretically possible routes for the synthesis of Cho: free base route, phospho (P) base route, cytidylyl (CDP) base route and phosphatidyl (Ptd) base route. The P-base route is shown with solid black arrows and is the biosynthetic pathway used by spinach. For simplification, arrows are unidirectional and do not preclude the operation of reverse reactions. The enzymes catalysing the reactions in spinach are also listed: ethanolamine kinase (EAK), phosphoethanolamine-*N*-methyltransferase (PEAMT) phosphomethylethanolamine-*N*-methyltransferase (PMEAMT), choline phosphatase (Cho PT), choline monooxygenase (CMO) and betaine aldehyde dehydrogenase (BADH)

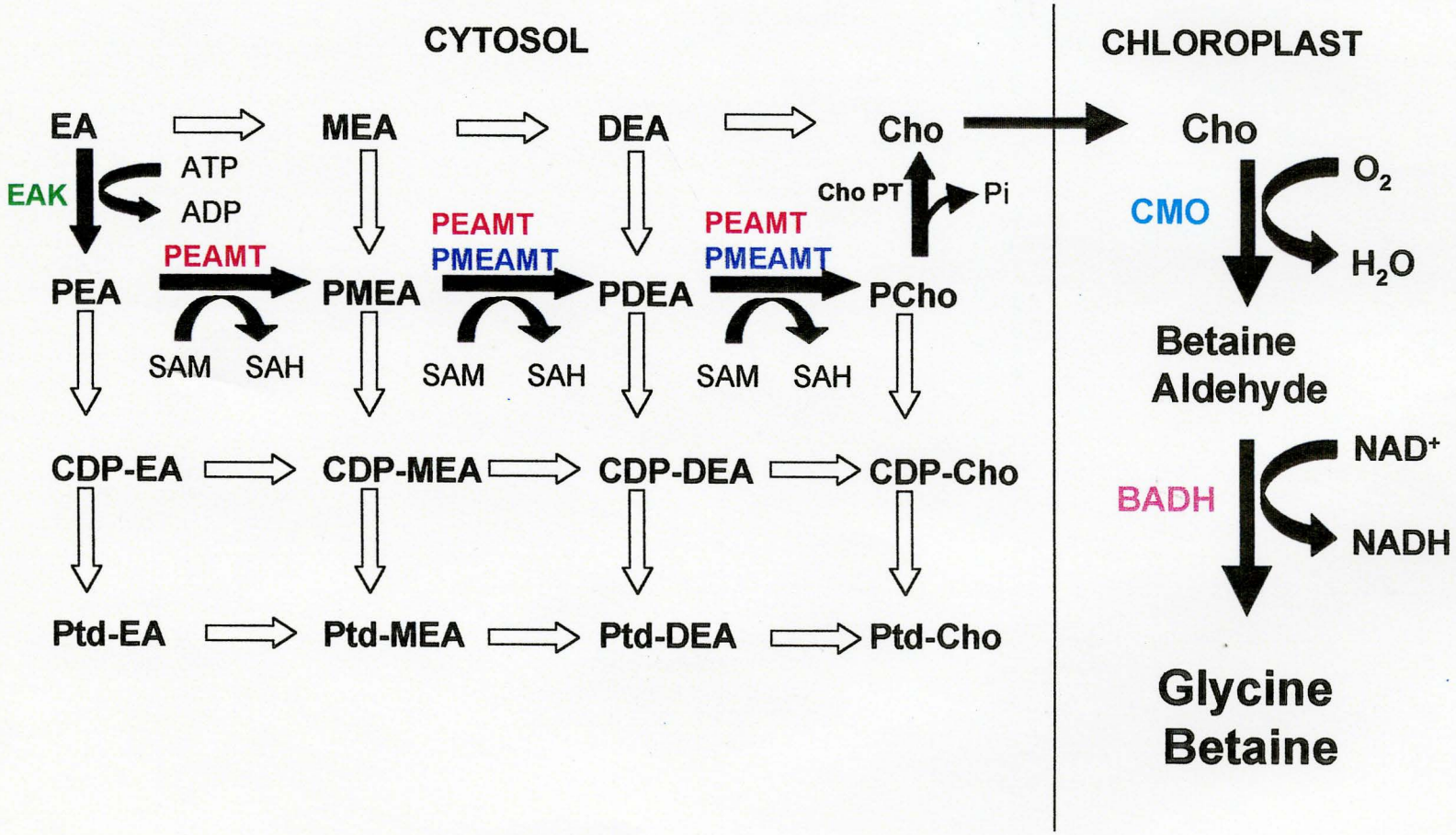
CYTOSOL
CHLOROPLAST
EA
MEA
DEA
Cho
EAK
ATP
ADP
Cho PT
Pi
PEAMT
PEAMT
PMEAMT
PEAMT
PMEAMT
PEA
PMEA
PDEA
PCho
SAM
SAH
SAM
SAH
SAM
SAH
CDP-EA
CDP-MEA
CDP-DEA
CDP-Cho
Ptd-EA
Ptd-MEA
Ptd-DEA
Ptd-Cho
Cho
CMO
O_2
H_2O
Betaine
Aldehyde
BADH
NAD^+
NADH
Glycine
Betaine

is specific for its substrate choline (Cho) with an apparent K_m of 0.1 mM towards this substrate (concentration of choline in chloroplasts is approximately 0.16 mM; Brouquisse *et al.*, 1989). CMO is a ferredoxin-dependent monooxygenase as it uses reduced ferredoxin as an electron donor (Brouquisse *et al.*, 1989). CMO activity, protein and mRNA levels are induced by salinity increasing 3 to 5-fold in the glycine betaine accumulator sugar beet (Russell *et al.*, 1998).

Betaine aldehyde dehydrogenase (BADH)

The second step in this pathway is catalysed by BADH, an enzyme that was first characterized from spinach leaves (Fig. 1; Arakawa *et al.*, 1987, Weretilnyk and Hanson, 1989). BADH is a dimer composed of subunits of approx 63 kD molecular mass and is found mainly in the chloroplast stroma, although there is a minor fraction in the cytosol (Weretilnyk and Hanson, 1988; Weigel *et al.*, 1986). With an apparent K_m of 2.08×10^{-4} M towards betaine aldehyde, spinach BADH is relatively specific for its substrate (Pan *et al.*, 1981) yet it also has a good affinity for several other aldehydes involved in polyamine metabolism (Trossat *et al.*, 1997). BADH is a pyridine nucleotide-dependent dehydrogenase and uses both NAD and NADP as cofactors, with a preference for NAD (Weretilnyk and Hanson, 1989). The reaction equilibrium lies in the direction of glycine betaine formation as the reverse reaction is not detected (Pan *et al.*, 1981). BADH activity increases with salt, and is accompanied by increases in BADH protein and mRNA levels (Weretilnyk and Hanson, 1989; Weretilnyk and Hanson, 1990).

The identification and characterization of enzymes involved in glycine betaine synthesis and the genes encoding them means that engineering an increased capacity for glycine betaine biosynthesis is a feasible target for genetic engineering of enhanced water deficit stress tolerance in stress sensitive plants (McCue and Hanson, 1990). Both tobacco (*Nicotiana tabacum*) and *Arabidopsis* have been transformed with transgenes that encode choline oxidizing enzymes including CMO (Hayashi *et al.*, 1997; Nuccio *et al.*, 1998). In the case of plants expressing active CMO and BADH, very little glycine betaine was produced by these plants when compared with levels of this QAC found in natural glycine betaine accumulators even when plants were salt stressed (Nuccio *et al.*, 1998). The reason as shown by Nuccio *et al.* (1998), was a smaller pool of endogenous choline in these plants. The authors proposed that for tobacco the supply of choline is the major limiting factor in glycine betaine synthesis (Nuccio *et al.*, 1998).

Choline Synthesis

Synthesis of choline begins with the production of free ethanolamine (EA) through the decarboxylation of serine (Mudd and Datko, 1989b; McNeil *et al.*, 2001). Figure 1 shows the possible pathways for the sequential methylation of EA as a free base, phosphobase (P-base) or phosphatidyl base (Ptd-base) (Rhodes and Hanson, 1993). Since many of the intermediates of these pathways are interconvertable, a complex picture of choline synthesis is created (Hitz *et al.*, 1981). The synthesis of choline also requires a significant input of energy given that synthesis of one molecule of PCho from EA requires 7 ATP (Hitz *et al.*, 1981; Weretilnyk *et*

al., 2001).

The P-base route of synthesis operates in some but not all glycine betaine accumulators (Hanson and Rhodes, 1983; Summers and Weretilnyk, 1993) EA is phosphorylated to phosphoethanolamine (PEA) by EA kinase using ATP (Fig 1). PEA may then be sequentially methylated to phosphomethylethanolamine (PMEA), phosphodimethylethanolamine (PDEA) and phosphocholine (PCho) using the methyl donor *S*-adenosyl-L-methionine (SAM). PCho is subsequently hydrolysed to choline by a choline phosphatase (Hitz *et al.*, 1981; Hanson and Rhodes, 1983). In barley, also a glycine betaine accumulator, Hitz *et al* (1981) have shown that following the conversion of PEA to PMEA, further *N*-methylations may proceed using both the P-base or the Ptd-base pathways. PtdCho is then hydrolysed thereby releasing choline (Hitz *et al.*, 1981).

Choline synthesis in plants that do not accumulate glycine betaine has also been investigated and differences in their pathways of choline synthesis have been reported. In a recent study by Lorenzin *et al.* (2001), 17 diverse plants were shown to share the capacity to *N*-methylate PEA and so to perform what is considered to be the committing step in the synthesis of choline (Hitz *et al.*, 1981; Mudd and Datko, 1989a; Lorenzin *et al.* 2001). Further *N*-methylations of PMEA occur at the P-base level in many of the plants studied to date but the Ptd-base pathway operates in soybean and pea and both P-base and Ptd-base levels in carrot and tobacco (Mudd and Datko, 1986; Datko and Mudd, 1988; McNeil *et al.*, 2000; Lorenzin *et al.*, 2001). An exception to the apparently common step involving the initial

methylation of PEA was provided by extracts of castor bean (*Ricinus communis*) endosperm. Prud'homme and Moore (1992) have published radiotracer evidence showing that EA is initially methylated to form methylethanolamine (MEA) and *N*-methylations subsequently continue along the free-base or the P-base pathways. However, Lorenzin *et al.* (2001) have found PEA *N*-methylating activity in the leaves of castor bean, showing that different organs may synthesize PCho differently. Leaves of plants studied to date show the same committing step for choline synthesis.

The regulation of choline synthesis is thought to reside at the site of the *N*-methylation of PEA to PCho. Thus the enzymes involved in catalysing these steps likely play important regulatory roles (Hanson and Rhodes, 1983). Hitz *et al* (1981) showed that the rate of choline synthesis depends on the size of the metabolically active pool of PCho. Supplying excised leaves of barley with 1 to 2 μmol PCho strongly reduced the *de novo* rate of synthesis of PCho and so reduced subsequent glycine betaine synthesis. When *Lemna paucicostata* was grown in 3 μM choline, PCho synthesis was similarly down-regulated as was the activity of SAM:P-base *N*-methyltransferases (Mudd and Datko, 1989b). The increase in choline levels in the *Lemna* fronds resulted in an 80% decrease in PEA *N*-methylation activity, with the rates of PMEA and PDEA *N*-methylation decreasing only 30% and 40%, respectively (Mudd and Datko, 1989b). Also, the activities of choline kinase and EA kinase were not affected. This reduction in PEA methylation was seen as highly specific and led Mudd and Datko (1989b) to suggest that the committing step to choline synthesis lay at this site. They proposed that

the down regulation of choline synthesis was caused by a decrease in the activity of the *S*-adenosyl-L-methionine dependent enzyme phosphoethanolamine *N*-methyltransferase (PEAMT), and that feedback inhibition of its activity from PCho might be responsible (Hanson and Rhodes, 1983; Mudd and Datko, 1989c).

PEAMT

PEAMT has been shown to catalyse all three sequential *N*-methylations of PEA to PCho (Fig 1; Smith *et al.*, 2000). PEA, PMEA and PDEA *N*-methyltransferase activities are salt-responsive in spinach plants salinized stepwise to 300 mM NaCl showing a 1.5 to 2-fold increase in activity over control plants (Summers and Weretilnyk, 1993). Salt shock with 200 mM NaCl leads to a 2-fold increase in each activity within 24 h (Weretilnyk *et al.*, 1995). This 2-fold-increase is comparable in magnitude to that seen in CMO and BADH activities upon salinization (Weigel, 1986; Brouquisse *et al.*, 1989).

PEAMT activity has also been assayed in spinach leaf extracts prepared from leaves harvested at various times during the diurnal photoperiod. Weretilnyk *et al.* (1995) showed the activity associated with the *N*-methylation of PEA was highest at the end of the light period and lowest following the dark period. Prolonged dark conditions further reduced PEAMT activity and return of plants to the light restored enzyme activity (Weretilnyk *et al.*, 1995). Moreover, the increase in activity following salt treatment is only seen in plants exposed to light. The *N*-methylation activities of both PMEA and PDEA were not observed to change similarly in response to light/dark treatment (Weretilnyk *et al.*, 1995). While no

measurable PEAMT activity exists in the roots of spinach, PMEA and PDEA *N*-methylation activities have been detected (Weretilnyk and Summers, 1992). The explanation for these observations lies in the existence of a second methyltransferase in this pathway which catalyses the *N*-methylations of PMEA and PDEA to PCho (Burian, 2000). The enzyme, designated PMEAMT, has been purified 7,507-fold from spinach leaves. Burian (2000) showed that two polypeptides are associated with PMEAMT activity; both polypeptides may be part of a single multimeric enzyme or possibly two different enzymes associated with this activity may exist (Burian, 2000).

Characterization of the properties of PEAMT has also been undertaken. Localization of the enzymes catalysing the three *N*-methylations of PEA to PCho was carried out by differential centrifugation of spinach leaf extracts and this showed all activities to be cytosolic (Weretilnyk *et al.*, 1995). PEAMT activity is optimal at pH 7.8 in HEPES-KOH buffer (Smith *et al.*, 2000). Using optimized assay conditions, PEAMT activity is inhibited by *S*-adenosyl homocysteine (SAH), PCho, phosphate, Mn^{2+} and Co^{2+} but not by EA, MEA, DEA, choline, glycine betaine or Mg^{2+} (Smith *et al.*, 2000). PEAMT has been partially purified 5,400-fold from spinach (Smith *et al.*, 2000). Separation of the mixture by sodium dodecyl sulfate-polyacrylamide gel electrophoresis (SDS-PAGE) and photo affinity crosslinking showed a single polypeptide with an estimated molecular mass of 54 kDa covalently cross-linked to [^{3}H]-SAM. A native molecular mass of 77 kDa was also determined by high performance liquid chromatography (HPLC) gel permeation chromatography (Smith *et al.*, 2000).

Photoaffinity crosslinking was used to show that PEAMT protein is more abundant in extracts of salinized plants than controls and plants in the light as opposed to plants in the dark where a cross-linking signal is barely visible (Smith *et al.*, 2000). Nuccio *et al.* (2000) isolated a PEAMT cDNA from spinach by complementation of a *Schizosaccharomyces pombe cho2*$^-$ mutant. This mutant lacks the enzyme that can methylate PtdEA to PtdMEA and requires MEA, DEA or choline for growth (Nuccio *et al.*, 2000). When this strain was transformed with the pREP3-based plasmid cDNA library prepared from salinized spinach plants, colonies growing in the absence of choline were recovered. Yeast cells rescued by this strategy were shown to share a plasmid bearing a specific cDNA and biochemical characterization of complemented strains indicated that they possessed PEAMT activity though wild type *S. pombe* does not (Nuccio *et al.*, 2000). The cloned cDNA was shown to encode a methyltransferase and the gene was designated *peamt*. Preliminary studies using the insert encoding *peamt* show that PEAMT mRNA levels increase in the leaves of salinized spinach plants (Nuccio *et al.*, 2000).

As a key enzyme in plant choline synthesis, PEAMT is a logical target for genetic engineering. McNeil *et al.* (2001) used a plant transformation construct encoding spinach PEAMT to transform a line of tobacco that co-expresses CMO and BADH. These transformants had high PEAMT protein levels, a 40-fold increase in PEAMT activity and up to 50-fold more free choline than controls. This greatly enhanced the capacity of tobacco to accumulate glycine betaine (about 30-fold). There was, however, a depletion of the EA and

PEA pools. McNeil *et al.* (2001) showed that when plants were supplied with exogenous EA there was a further increase in choline levels. Thus engineering to increase the EA supply is also necessary for glycine betaine to accumulate to high levels in transgenic plants.

Circadian Rhythms

Circadian rhythms are found in bacteria, fungi, plants and animals (McClung, 2001). In plants, diverse processes are controlled by circadian rhythms, both at the organismal level and molecular level and covering a broad range of processes including flower opening in the morning and photosynthesis (Hennessy and Field, 1991; Somers, 1999). The internal circadian rhythm of the plant becomes synchronized to the cycle(s) of the external environmental conditions it is exposed to in a process called entrainment (Raven *et al.*, 1999). Depending on the environmental conditions, circadian rhythms can be entrained or "set" to differing lengths of each cycle or "period" and rhythms within the cycle or "phases" (Kreps and Simon, 1997). While these endogenous rhythms oscillate with a nearly 24 h periodicity (hence circa-dian meaning 'about a day'), a key feature of a circadian rhythm is that it persists even when environmental conditions responsible for entrainment are changed (Kreps and Simon, 1997; McClung, 2000). Circadian oscillations observed in plant processes are thought to be generated by a central oscillator(s) whose characterization is ongoing (Kreps and Simon, 1997; McClung, 2001). Circadian rhythms allow anticipation of daily events such as dawn and dusk thereby providing adaptive fitness (McClung, 2001; Kondo *et al.*, 1994). For example, increased growth and developmental rate has been reported for some plants maintained at

their normal light/dark cycle over those subjected to constant light (Ouyang *et al.*, 1998).

The basic model of the plant circadian system has been divided into three parts: the **inputs,** the **central oscillator(s)** and the **outputs** (Fig. 2; McClung, 2001; Merrow *et al.*, 1997). Inputs are the environmental cues, such as light and temperature, that entrain the central oscillator(s) to a specific period length (Somers, 1999). The central oscillator(s) link the external environmental inputs to the outputs such as rhythms seen in plant physiology and development. Output pathways include signal transduction pathways that control obvious or overt rhythms seen in different circadian-regulated processes (Somers, 1999). Current research in this area is concerned with identifying possible genes and proteins operating within the system and positioning them as an input, central oscillator or output (Hartwell *et al.*, 1996; Johnson *et al.*, 1998).

Input to the clock

Light

Entrainment of the circadian clock by light is well understood (McClung, 2000). How a plant perceives light has been studied in detail revealing the involvement of photoreceptors. Photoreceptors are able to distinguish quality of light and they include the phytochromes (red light receptors) and the cryptochromes (blue light receptors) (Millar *et al.*, 1995; Finlayson *et al.*, 1999). An *Arabidopsis* mutant deficient in all five phytochromes shows a longer period in its central oscillator(s) under conditions of red and white light than wild-type plants. A similar lengthening of period is seen with cryptochrome mutants under

FIGURE 2: Model of the circadian system

This model of the circadian system has been adapted from one proposed by McClung (2001). The basic model of the circadian system in plants shows the input pathways, central oscillator(s) and output pathways. Each component contains many signal transduction pathways that may, in turn, interact with the other two components. This complex level of interaction cannot be shown in a simplified figure. The sun is important in that it impacts on the two main inputs, namely light and temperature, and it cycles with an approximate 24 h period. External environmental changes such as light and temperature that cycle are perceived by the plant by receptors and input pathways then serve to entrain the central oscillator(s). The central oscillator(s) is shown as several loops of forward reactions and inhibited reactions, that can interact with each other. The rhythm(s) generated in the central oscillator(s) give rise to the output pathways that cause the apparent or overt rhythms seen in different plant processes. Not shown is the potential for the central oscillators to generate rhythms of different period lengths.

Input
Pathways
Central
Oscillator(s)
Output
Pathways
Overt
Rhythms
Light
phytochromes
cryptochromes
Temperature
temperature
sensors

conditions of blue light (Somers, 1998). Phase shifts in the rhythms of many processes can also be caused by varying light quality or quantity. Wheat exposed to light pulses lasting approximately 3 h show a shift in the rhythms of gene expression (Nagy *et al.*, 1993). Thus changes in light quality and quantity are monitored by plants and changes in circadian rhythms are seen as a consequence.

Temperature

The circadian oscillator can also be entrained by the cycling of different temperatures (McClung, 2001). Rhythmic changes in temperature can be a stronger entraining mechanism than light in some processes (Somers, 1999). In crassulacean acid metabolism (CAM) plants kept at 20°C, phosphoenolpyruvate carboxylase kinase (PEPC-kinase) mRNA abundance shows a circadian rhythm with peak abundance during the night. Lowering the temperature to 4°C delays the decrease in mRNA during the day. Conversely, raising the temperature to 30°C accelerates the decrease in mRNA abundance such that the change in temperature alters the phase of the rhythm (Wilkins, 1992). The clock has also been shown to stop when chilling-sensitive plants are exposed to pulses of cold (Jones *et al.*,1998).

Photoreceptors and temperature sensors initiate entrainment of the clock (Somers, 1999). Signal transduction pathways that convey this information to the clock are not well understood. However, new component proteins of the pathways are being discovered and characterized through investigations of genes shown to oscillate and/or through a closer study of the proteins they encode (Kreps and Simon, 1997; Heintzen *et al.*, 1997).

Central oscillator

Components of the central oscillator include factors regulating the cycling transcription of key clock genes and the subsequent rhythm in the abundance or activity of their gene products. The oscillations in these components are generated because it takes time for the protein product(s) to 'feed back' either positively or negatively to influence the transcription of the genes encoding them. An example of a delay would be the time needed for these factors to reach the nucleus from subcellular sites where they originate to feed back inhibit or induce gene transcription (Dunlap, 1999). The molecular details of this process are unknown (McClung, 2000).

Evidence can now be found for the occurrence of multiple clocks within an organism and indeed a single cell (Fig. 2; Roenneburg and Morse, 1993; Kolar *et al.*, 1995). The existence of two distinct oscillators has been shown in the unicellular alga *Gonyaulax polyedra* (Morse *et al.*, 1994). In plants, examples exist where different organs have processes differing in period lengths as seen by the differing rhythms of stomatal aperture and leaf movement in *Phaseolus vulgaris* (Hennessy and Field, 1992). Differing periods indicates that either two central oscillators exist or different oscillators are present in different organs (Hennessey and Field, 1992). Also, in *Arabidopsis* and tobacco seedlings one cotyledon could be entrained to a different phase than the other, even while the shoot apex retained the original phase (Thain *et al.*, 2000). Therefore, multiple oscillators can exist in individual plants and they may or may not interact with each other.

Outputs

Outputs with a circadian rhythm are seen at the organismal and molecular level. At the plant level, studies on the pulvinar sleep movements of leaves are well known (McClung, 2000). Here cells in the extensor and flexor regions of the pulvinus swell with opposing phases in a circadian period thereby driving the daily changes in leaf position (Engelmann and Johnsson, 1998). Molecular systems with circadian rhythms include many processes such as photosynthesis as described earlier for PEPC-kinase in CAM plants and for hormone levels such as ethylene production (Somers, 1999; McClung, 2001). The number of genes found to be circadian-regulated is continually growing (Somers, 1999). Microarray analysis permits the identification and examination of circadian oscillations in transcript abundance on a 'global' scale and thus revealing patterns of gene expression displaying circadian control (Dunlap, 1999; Harmer *et al.*, 2000). Harmer *et al.* (2000) has recently reported 453 genes in *Arabidopsis* that cycle. Possibly universal among angiosperms is the example of the chlorophyll a/b binding protein gene (LHCb) which has oscillating mRNA abundance due to clock-regulated transcription (Harmer *et al.*, 2000). Many genes encoding proteins involved in photosynthesis are cycling and peak between dawn and mid-day; LHCb transcript levels peak before dawn (Somers *et al*,. 1998). Maximal transcript levels of different genes can occur at distinct circadian phases (Harmer *et al.*, 2000). In *Arabidopsis* the mRNA abundance of the catalase encoding genes *cat2* and *cat3* peak at dawn and dusk, respectively (McClung, 2001). Post-transcriptional control of these circadian-regulated genes can either obscure or

contribute to oscillations in mRNA abundance by affecting the abundance of protein products (Somers, 1999). The rhythm in nitrate reductase mRNA abundance in *Arabidopsis* shows post-transcriptional control since nuclear run-on experiments were not able to detect transcript oscillations (Pilgrim *et al.*, 1993). Post-translational control can also obscure oscillations in transcript abundance or produce oscillations in protein level or activity where there is none for the transcript. One example lies in enzyme phosphorylation which is increasingly shown as a mechanism of circadian post-translational regulation causing the activity of enzymes such as PEPC-kinase and sucrose phosphate synthase to show circadian oscillations in activity (Jones and Ort, 1997).

MATERIALS AND METHODS

Chemicals and enzymes used were purchased from Sigma (Sigma-Aldrich Canada Ltd., Oakville, Ontario) unless noted otherwise. Water used to prepare reagents was purified by a Barnstead NANOpure II water purification system (SYBRON/Barnstead, Boston, Massachusetts). The substrate *S*-adenosyl-L-methionine (SAM) (Roche Diagnostics, Laval, Quebec) was dissolved in 0.01 N H_2SO_4: ethanol 9:1 (v/v). The absorbance of the solution was measured spectrophotometrically at 257 nm and used to calculate the concentration of SAM using the molar extinction coefficient of 15 M^{-1} cm^{-1} (Eloranta et al., 1976).The solution was then diluted to 12 mM with 0.01 N H_2SO_4: ethanol 9:1 (v/v), dispensed into 25-µL aliquots and stored at -20°C until required. *S*-[methyl-^{3}H]adenosyl-L-methionine ([^{3}H]SAM) (NEN™ Life Science Products, Inc., Boston, Massachusetts) was purchased as a 10 mM solution in H_2SO_4: ethanol 9:1 with a specific activity of 85 Ci $mmol^{-1}$. PEA (Cat. No. A7007, Sigma) substrate was dissolved in 0.01 N HCl to a final concentration of 7.5 mM and stored at -20°C. DOWEX 50W (H^+) X8-200 resin (J.T. Baker, Phillipsburg, New Jersey) was regenerated by resuspending 300 g of resin in approximately 600 mL of 1 N HCl. The resin was allowed to settle and the HCl was decanted and discarded. This process was repeated at least 30 times in order to completely protonate the resin. Removal of excess HCl was accomplished by resuspending the resin with H_2O, allowing it to settle and decanting off the H_2O. This wash with H_2O was repeated until the pH of the H_2O decanted from the resin was between 6 and 7 (about 40 times).

peamt cDNA CLONE MODIFICATION

A cDNA clone encoding spinach PEAMT was obtained from Dr. Andrew D. Hanson, U of Florida as a plasmid preparation. The cDNA insert was cloned in the *Schizosaccharomyces pombe* expression vector pREP3-B (Nuccio *et al.*, 2000).

Polymerase Chain Reaction (PCR)

The *peamt* cDNA was amplified by PCR using the forward primer 5'-GTGTTACCATGGCCGCTTCAG-3' (AB21127) and the reverse primer 5'-CGGGATCCTGCTTTCACCAGCTC-3' (AB21289). These primers were designed by Drs. Elizabeth Weretilnyk and Barbara Moffatt and synthesized at the Central DNA Facility, McMaster University. Analysis of the primers was performed using the "Oligo Calculator" (www.pitt.edu/~rsup/OligoCalc.html). This program helps determine the concentration and optimal oligonucleotide annealing temperatures for PCR reactions (756.0 pmol μL^{-1}, 50°C for the forward primer and 748.5 pmol μL^{-1}, 61°C for the reverse primer). These primers were designed to introduce several nucleotide changes in the *peamt* coding sequence resulting in the creation of the restriction sites *Nco* I at the putative translational initiation site and *Bam*H I at the end of the longest open reading frame (for changes see Appendix 1a). The PCR reaction mixture contained final concentrations of 1 pmol μL^{-1} each of forward and reverse primers, 1 x PCR buffer (containing 20 mM Tris-HCl pH 8.8 (Tris (hydroxymethyl) aminomethane), 10 mM KCl, 10 mM $(NH_4)_2SO_4$, 2 mM $MgSO_4$, 0.1% Triton X-100, 0.1 mg mL^{-1} bovine serum albumin (BSA); Invitrogen Corporation, Rockville, Maryland), 0.2 mM

dNTP mix (Invitrogen), 20 mM $MgCl_2$ (Invitrogen), 1 μL of purified pREP3-B vector containing the *peamt* cDNA insert, and 0.5 μL DNA polymerase (Stratagene, La Jolla, California). PCR reactions were performed using a GeneAmp PCR System 2400 Thermocycler (Perkin Elmer, Wellesley, Massachusetts) with denaturation at 94°C, 3 annealing cycles at 50°C and 30 annealing cycles at 61°C. Alternatively, more stringent annealing conditions were used eliminating the 3 annealing cycles at 50°C for amplification of insert already modified with the *Nco* I and *Bam*H I restriction sites. DNA amplified by PCR was then precipitated with 2.5 vol absolute ethanol (Commercial Alcohols Inc., Brampton, Ontario) and 0.1 vol 3 M sodium acetate at -20°C overnight. The precipitated DNA was recovered by centrifugation at 14,000 *g* for 5 min and the pellet was dissolved with 20 μL sterile H_2O (Invitrogen).

Non-denaturing Gel Electrophoresis

DNA was separated by electrophoresis on a 1.2% (w/v) agarose gel containing 0.05 μg mL^{-1} ethidium bromide (Roche Diagnostics). The desired quantity of DNA was mixed with 2 μL of bromophenol blue running dye containing 0.2% (w/v) bromophenol blue, 60% (v/v) glycerol and 60 mM EDTA (ethylenediaminetetraacetic acid, disodium salt) and loaded on the gels. One lane was reserved for 5 μL 4-fold diluted λ DNA/ *Hind* III Marker 2 DNA molecular weight standards (Cat. No. SM0101, MBI Fermentas Inc., Burlington, Ontario) also mixed with 1 μL running dye. Gels were electrophoresed in a Bio-Rad Mini-Sub Cell GT apparatus (Bio-Rad Laboratories, Hercules, California) at 60 V for 1.5 h with a 1 x TAE

buffer (10x Stock contains 0.4 M Tris-acetate pH 8.0, 0.01 M EDTA, 0.2 M sodium acetate) and the bands visualized using long-wave UV light on a transilluminator (312 nm Variable Intensity Transilluminator; Fisher Scientific Biotech, Nepean, Ontario). Photographs of these gels were taken using a Cosmicar video system (COHU High Performance CCD camera; Mandel Scientific, Guelph, Ontario) and a Mitsubishi video copy processor (Mandel). The approximate size of the DNA in each band was determined by comparison to position of the bands associated with the λ DNA/ *Hind* III Marker 2 molecular weight standards.

Restriction enzyme digestion of DNA

Both PCR-amplified *peamt* insert and pET30a (+) vector (Novagen, Madison, Wisconsin; without insert) were dissolved in H_2O and subjected to restriction enzyme digestion with *Nco I* and *Bam*H I (Roche Diagnostics and Invitrogen, respectively). The digestion reaction mixture included 10 µL of DNA (approximately 5 µg), 0.5 µL *Nco* I, 0.5 µL *Bam*H I, 3 µL React Buffer 3 (Invitrogen) and 6 µL H_2O and was incubated at 37°C for 120 min. The restriction digestion products were precipitated with 2.5 vol absolute ethanol and 0.1 vol 3 M sodium acetate at -20°C overnight. The precipitated DNA was recovered by centrifugation at 14,000 *g* for 5 min and the pellet was dissolved in 12 µL sterile H_2O. These restricted cDNA inserts and plasmid preparations could then be used in ligation reactions.

INSERT DNA PURIFICATION AND LIGATION REACTIONS

The *peamt* cDNA insert was ligated into the expression vector pET30a (+). This plasmid has a T7 *lac* promoter and carries a N-terminal polyhistidine-tag as well as a marker

gene for kanamycin resistance (Appendix 1 b). pET30a (+) and DNA insert encoding *peamt* were prepared for ligation by restriction enzyme digestion and purification as above. The ligation mixture contained 12 μL (35 ng μL^{-1}) PCR amplified insert, 1 μL (135 ng μL^{-1}) pET30a (+), 4 μL 5x DNA ligase reaction buffer (250 mM Tris-HCl pH 7.6, 50 mM $MgCl_2$, 5 mM ATP, 5 mM DTT (DL-dithiothreitol), 25% (w/v) polyethylene glycol-8,000; Invitrogen), 1 μL T4 DNA ligase (in 10 mM Tris-HCl pH 7.5, 50 mM KCl, 1 mM DTT, 50% (v/v) glycerol; 100 Units, Cat No. 15224-017, Invitrogen) and 2 μL H_2O. The ligation reaction was incubated overnight at 15°C.

TRANSFORMATIONS AND SCREENING

Ligation products were used to chemically transform an *E.coli* host strain DH5α, a strain that lacks the gene for T7 RNA polymerase. One mL of LB media (containing 10% (w/v) Bacto-tryptone, 5% (w/v) Bacto-yeast extract, 10% (w/v) NaCl; adjusted to pH 7 with 5 N NaOH) was inoculated with a single colony of DH5α and incubated overnight at 37°C with shaking (200 rpm) in an Innova 4300 incubator shaker (New Brunswick Scientific Co., Inc., Edison, New Jersey). 100 μL of this overnight culture was then used to inoculate 50 mL LB which was incubated for 2 h at 37°C with shaking (200 rpm). This culture was centrifuged in an Avanti J-25 centrifuge (Beckman-Coulter Instruments, Fullerton, California) at 3,000 *g*, 4°C for 5 min. The supernatant was decanted and the cells were kept at 4°C or on ice from this point on. The cells were resuspended with 5 mL of ice-cold 0.1 M $MgCl_2$ and centrifuged at 3,000 *g* for 5 min. The supernatant was discarded and 10 mL of ice cold 0.1

M $CaCl_2$ was added to resuspend the cells. The cell suspension was incubated on ice for 20 min then the cells were pelleted by centrifugation at 3,000 *g* for 5 min. After discarding the supernatant, 1 mL of 0.1 M $CaCl_2$ was used to resuspend the pellet and 200 µL of this suspension was transferred to a round bottom polypropylene tube (Cat. No. 4-2059-2, Falcon®, Becton Dickinson Labware, Lincoln Park, New Jersey). 5 µL of ligation reaction product were added and the mixture allowed to incubate on ice for 40 min. The cells were heat-shocked at 42°C for 3 min before 1.8 mL of SOC medium (containing 2% (w/v) Bacto-tryptone, 0.5% (w/v) Bacto-yeast extract, 10 mM NaCl, 2.5 mM KCl, 10 mM $MgCl_2$, 10 mM $MgSO_4$, 20 mM glucose) was added and the cells incubated for 2 h at 37°C with shaking (200 rpm). The BL21(DE3) *E. coli* host strain (Novagen) was transformed using the same chemical transformation protocol. BL21(DE3) can induce expression of genes cloned in pET plasmids because it provides a source of T7 RNA polymerase.

Following transformation, DH5α or BL21(DE3) cells were plated to select for those cells transformed with the *peamt* cDNA insert. 100 µL of cells were diluted 10^{-1}, 10^{-2}, and 10^{-3}-fold in liquid LB media. 100 µL of each dilution was plated on solid LB media (liquid LB containing 1.5% (w/v) agar) containing 30 µg mL^{-1} kanamycin. Plates were incubated at 37°C overnight. Several colonies were picked from the plates and each colony was streaked with a sterile toothpick onto individual squares of a plate divided into grids and then the same toothpick was used to inoculate 10 µL PCR grade H_2O (Invitrogen). As many as 10 colonies were used to inoculate each tube of H_2O allowing for the pooled analysis of 10 colonies by

each PCR reaction. These pools of colonies suspended in H_2O were subjected to a modified PCR reaction in which 0.05% (v/v) Tween 20 (polyoxyethylene-sorbitan monolaurate) was added to lyze the cells. Primers and PCR reaction conditions were as outlined earlier. PCR products were separated by electrophoresis to identify the pool(s) showing a band corresponding to the size of the insert (1.5 Kb). Pools testing positive for the presence of a 1.5 Kb insert were analysed further by isolating plasmid DNA from each colony making up the pool using the Wizard *Plus* SV Minipreps DNA Purification System kit (Promega, Madison, Wisconsin) following the manufacturer's protocol. Plasmids were then subjected to restriction enzyme digestion with *Nco* I and *Bam*H I and the products separated by electrophoresis on a 1.2% (w/v) agarose gel, as outlined earlier, to identify transformants with the desired insert. A single plasmid was selected and insert sequence was verified by sequencing the cDNA using the T7 promoter and terminator primers (performed by the Central DNA Facility, McMaster University; Appendix 1 c). The pET30a(+) plasmid containing insert was used in a chemical transformation of BL21(DE3).

***peamt* EXPRESSION**

BL21(DE3) transformed with pET30a (+) containing *peamt* cDNA was induced to express *peamt* using the pET30a (+) expression system protocol (pET System Manual, http://www.novagen.com/SharedImages/TechnicalLiterature/7_tb055.pdf). Bacteria were grown in 50 mL LB liquid media at 37°C with constant shaking (200 rpm). When the culture reached an OD_{600} of 0.6 (measured with a UVIKON 950 spectrophotometer, Kontron

Instruments, Zürich, Switzerland), IPTG (isopropylthio-β-D-galactoside) was added to a final concentration of 0.4 mM and incubation continued for a further 2 h. Flasks were then placed on ice for 5 min, and cells harvested by centrifugation at 5,000 *g* for 5 min at 4°C. The supernatant was saved and stored at -20°C. The pellet was resuspended with 0.25-culture volumes of buffer containing 50 mM HEPES-KOH pH 7.8 (hydroxyethylplperazine-N'-2-ethanesulfonic acid), 5 mM DTT and 1 mM EDTA and centrifuged again. The pellet was resuspended with 500 μL of buffer as above. The cells, in suspension, were broken by sonication using a Branson Sonifier Cell Disruptor 350 (Branson Sonic Power a SmithKline Company, Danbury, Connecticut). The broken cells were centrifuged at 14,000 g for 10 min at 4°C and the supernatant retained as a cell-free extract, flash frozen and stored at -80°C.

PURIFICATION OF EXPRESSED PROTEINS BY CHROMATOGRAPHY ON METAL AFFINITY RESIN

PEAMT protein bearing the polyhistidine tag was purified from bacterial cell-free extracts using a cobalt metal affinity resin column (Talon®; Clontech, Palo Aito, California) as a batch-wise, gravity flow column purification according to the manufacturer's instructions. Talon® resin uses Sepharose® CL-6B beads provided as a 50% (w/v) slurry in 20% (v/v) ethanol. The resin was resuspended by swirling and 2 mL was transferred to a 15 mL conical tube (Falcon®, Becton Dickinson Labware), the beads were allowed to settle and the supernatant discarded. 10 mL of extraction/wash buffer containing 50 mM HEPES-KOH pH 7.8, 300 mM NaCl and 10 mM β-mercaptoethanol were added to pre-equilibrate the resin.

The resin beads were pelleted by centrifugation at 700 *g* for 2 min at room temperature and the supernatant was discarded. A maximum of 17 mg of protein in 600 µL of buffer (50 mM HEPES-KOH pH 7.8, 5 mM DTT and 1 mM EDTA) were diluted 15-fold with extraction/wash buffer and the entire volume was added to the resin. The mixture was gently agitated at room temperature for 20 min to allow the polyhistidine-tagged protein to bind to the resin and then the resin/protein complex was pelleted as described above. The beads were washed by gentle agitation in 10 mL of extraction/wash buffer for 10 min at room temperature and then removing the liquid by pelleting the resin. This procedure was repeated two more times and the supernatants from all of the washes were retained. Next, 1 mL of extraction/wash buffer was used to resuspend the resin which was then transferred to a poly prep column (Evergreen Scientific, Los Angeles, California) and the beads allowed to settle. The buffer was drained and the column contents were washed with 5 mL of extraction/wash buffer. The last wash was followed with 5 mL extraction/wash buffer containing 5 mM imidazole. Polyhistidine-tagged proteins were then eluted from the matrix by adding 5 mL of elution buffer containing 50 mM HEPES pH 7.8, 300 mM NaCl, 150 mM imidazole and 10 mM β-mercaptoethanol. Fractions of 500 µL volume were collected in 1.5 mL microfuge tubes and polypeptides eluted from the column were analysed by electrophoresis on SDS-polyacrylamide gels (see Materials and Methods section entitled "SDS-polyacrylamide gradient gel electrophoresis").

PREPARATION OF POLYCLONAL ANTIBODIES

Polyhistidine-tagged PEAMT was used to raise polyclonal antibodies in a rabbit (New Zealand White) under the McMaster University Animal Utilization Proposal assigned to Dr. Elizabeth Weretilnyk (AUP # 00-05-17). All animal work was kindly done by the staff at the Central Animal Facility (CAF). Blood samples (pre-immune or post-immunization) were allowed to clot for 30 - 60 min at 37°C and then the clot was allowed to contract overnight at 4°C. After centrifugation at 10,000 g for 10 min at 4°C, the clear serum was removed and stored at -20°C in aliquots of 500 µL. Polyhistidine-tagged PEAMT protein from the Talon column was desalted by centrifugation through Sephadex™ G-25 (Amersham-Pharmacia Biotech, Baie d'Urfé, Québec) equilibrated in 0.85% sterile saline solution (0.85% (w/v) NaCl). Approximately 200 µg mL^{-1} protein in a 500 µL preparation was emulsified with an equal volume of Freund's Complete Adjuvant (Cat. No.F-5881, Sigma) for the first injection. A booster injection of similarly prepared protein emulsified in an equal volume of Freund's Incomplete Adjuvant (Cat. No.F-5506, Sigma) was given 4 weeks following the first immunization. Blood was collected 4 times; once after the initial injection and three times after the booster injection.

ANTIBODY TITRE

Antibody titre was evaluated by dot blot immunoassay analysis using a Bio-Rad Bio-Dot® Microfiltration Apparatus and following the manufacturer's protocol for protein blotting. A nitrocellulose membrane (Schleicher and Schuell, Inc., Keene, New Hampshire) was pre-wetted in Tris buffered saline (TBS; 20 mM Tris, 150 mM NaCl). The membrane was

re-hydrated in the apparatus by applying 100 µL TBS to all 96 wells and allowing it to filter through the membrane under vacuum. The antigen was diluted to equal final volumes containing 100, 50, 40, 20, 10 and 5 ng protein. These samples were diluted in HEPES buffer (50 mM HEPES-KOH pH 7.8, 5 mM DTT and 1 mM EDTA) and applied directly to the membrane (hence "native") or applied after the samples were SDS-denatured by dilution in TBS containing 0.1% (w/v) SDS and heated for four min at 90°C (hence "denatured"). The antigen was allowed to filter through the membrane by gravity. After "blocking" the membrane by gravity filtration with 1% (w/v) BSA in TBS, the membrane was washed with 200 µL TBS + 0.05% (v/v) Tween 20 (TTBS) per well by vacuum filtration. Antibody sera diluted 1,000-fold in antibody dilution buffer (1% (w/v) BSA in TTBS) was then applied to the wells. Each blood collection (pre-immune, collections 1, 2, 3 and 4) were tested. When the dilute antibody had drained by gravity flow the membrane was washed three times with 200 µL TTBS per well. The secondary antibody (affinity purified goat anti-rabbit IgG (H+L) alkaline phosphatase conjugate; Cat. No. 170-6518, Bio-Rad) was diluted with antibody dilution buffer 3,000-fold and 100 µL was applied to each well. When the antibody had drained by gravity flow the membrane was washed three times with 200 µL TTBS per well. The membrane was then removed from the apparatus and washed two times with 100 mL TBS. The blot was developed using a colour development solution (BCIP/NBT colour developer described by Sambrook *et al.*, 1989). The development reaction was stopped by several washes with water and then the membrane was air dried.

ANALYSIS OF PEAMT ACTIVITY, PROTEIN, AND TRANSCRIPTS IN SPINACH

Plant material

Spinach (*Spinacia oleracea* L. cv. Savoy Hybrid 612) seeds (Harris Moran Seeds, Rochester, NY, USA) were germinated in flats of coarse vermiculite and seedlings were transplanted after 1 week to individual 350-mL plastic pots of vermiculite. Plants were grown under an 8 h/24°C light, 16 h/19°C dark photoperiod with photosynthetically active radiation (PAR) at 350 μmol m^{-2} s^{-1}. Plants were irrigated with half-strength Hoagland's solution (Hoagland and Arnon, 1950) or with the same solution supplemented with NaCl for salt treatments. Step-wise salinization of plants to a final concentration of 200 mM NaCl began 4 weeks post-germination, starting with 50 mM NaCl and increasing the salt concentration every three days by 50 mM increments to a final concentration of 200 mM.

For light treatments, five-week-old plants were placed in continuous light or dark (depending on the experiment). Unless otherwise specified, half to fully expanded leaves from at least two plants were harvested at four-hour intervals. Leaves were coarsely chopped with a razor blade and a sample of tissue equivalent to 2 g fresh weight was used in the preparation of a crude extract. The remaining tissue was immediately frozen in liquid N_2 and stored at -80°C until total RNA could be isolated. Crude leaf extracts were prepared at 4°C or on ice. Tissue was ground in a cold mortar with a pestle and a small amount of sea sand with a buffer containing 50 mM HEPES-KOH pH 7.8, 5 mM DTT and 1 mM EDTA (2 mL g^{-1} fresh weight). The brei was centrifuged at 10,000 *g* for 10 min, the supernatant was

dispensed into 1 mL aliquots, the tubes flash frozen in liquid N_2 and stored at -80°C. Dr. Peter Summers maintained the plants, applied many of the treatments and also helped with the harvesting of plants.

PEAMT enzyme assay

Crude extracts prepared as described above were thawed and desalted by centrifugation through Sephadex G-25 Medium equilibrated with grinding buffer (Summers and Weretilnyk, 1993). PEAMT activity was assayed as described by Summers and Weretilnyk (1993). Each assay consisted of 100 µL of PEAMT assay buffer (150 mM HEPES-KOH pH 7.8, 1.5 mM EDTA), 2.5 µL of 12 mM SAM, 1 µL of [^{3}H] SAM (0.55 µCi; 1.22 x 10^6 dpm), 21.5 µL H_2O, 5 µL of 7.5 mM PEA substrate (or water in control assays) and 25 µL of sample extract to a final assay volume of 150 µL. Upon addition of the sample extract, the mixture was gently vortexed to mix and the assay incubated in a water bath at 30°C for 30 min. Addition of 1 mL ice-cold H_2O was used to stop the reaction and the mixture was vortexed to mix and the tubes placed on ice. A 1-mL aliquot of the diluted reaction was applied to a disposable column containing a 1-mL bed volume of DOWEX 50W (H^+) X8-200 resin. The column matrix was washed three times with 0.5 mL H_2O each time. P-bases bound to the Dowex resin were eluted from the resin with 10 mL of 0.1 N HCl. The eluate was vortexed to mix and 1 mL was transferred to a vial containing 5 mL Ready Safe® fluor (Beckman-Coulter Instruments Inc.), vortexed, and the radioactivity quantified with a Beckman LS 1801 liquid scintillation counter (Beckman-Coulter Instruments Inc.). Counting

efficiency for ^{3}H using this fluor was determined previously to be 41.6% (unpublished). When counts per min (cpm) exceeded 3,000, sample extracts were diluted up to 200-fold using the grinding buffer and the assay performed again in order to ensure linearity of the assay. A concentration of 10 nM SAH, a reaction product, has been reported to inhibit PEAMT activity by 53% relative to uninhibited controls (Smith *et al.*, 2000).

Protein concentration

The protein concentrations of sample extracts were determined by the method of Bradford (1976) using the Bio Rad Protein Assay Dye Reagent Concentrate (Bio-Rad) following the manufacturer's protocol. The colorimetric change in absorbance was monitored at 595 nm using the spectrophotometer. Protein concentration was estimated by comparison of the absorbance readings of the samples with those of a standard curve generated using known concentrations of BSA.

SDS-polyacrylamide gradient gel electrophoresis

Sample extracts were separated by electrophoresis on a 7.5-15% SDS-polyacrylamide gradient gel using the buffer system described by Nelville (1971). Extracts were mixed with an equal volume of SDS-solubilizing buffer (60 mM Tris-HCl pH 6.8, 10% (v/v) glycerol; 1% (w/v) SDS, 1% (w/v) DTT and 0.002% (w/v) bromophenol blue) and heat-denatured at 90°C for 3 min. For Mr determination, polypeptides of known Mr (Bio-Rad SDS-PAGE low range molecular weight kit) were diluted with SDS-solubilizing buffer (at a ratio of standards: solubilizing buffer of 1:20 for gels stained with Coomassie dye or 1:100 for gels stained with

silver reagent) and then heated as described above. Electrophoresis was performed at 15 mamp/1.5 mm gel thickness at 15°C until the bromophenol blue dye marker migrated to 0.5 cm from the bottom of the gel (approximately 4 h).

When electrophoresis was complete, gels were stained with a Coomassie dye or silver reagent to reveal the polypeptides. Coomassie staining involved soaking the gels in a solution of 0.1% (w/v) Coomassie Brilliant Blue R250, 25 % (v/v) isopropanol, 10% (v/v) glacial acetic acid and 0.1% (w/v) cupric acetate overnight with gentle agitation. Destaining was completed by gentle agitation in 40% (v/v) methanol and 7% (v/v) glacial acetic acid using foam plugs to speed the removal of excess dye. Gels to be stained with silver reagent were soaked in 50% (v/v) reagent grade methanol overnight and then stained following the method of Wray *et al.* (1981). Both Coomassie dye and silver stained gels were soaked for 2 h in gel drying solution (40% (v/v) methanol, 7% (v/v) glacial acetic acid, and 3% (v/v) glycerol). Gels were air dried between two sheets of cellophane (Bio-Rad) (Wallevik and Jensenius, 1982).

Immunodetection of PEAMT protein

Coupling antibodies to protein A agarose beads

Polyclonal antibodies were covalently linked to protein A agarose beads (Cat. No. 1719 408, Roche Diagnostics). Protein A agarose beads are supplied as a 1:1 suspension in 10 mm sodium phosphate with 400 µL of the suspension yielding approximately 200 µL settled volume of beads. The beads were resuspended with 400 µL phosphate buffered saline

(PBS, 10 mM sodium phosphate pH 7.2 and 0.9% (w/v) NaCl) and centrifuged for 5 s at 14,000 *g* to pellet the beads. The supernatant was discarded and the wash with PBS repeated. 20 µL of PEAMT antiserum (equivalent to 2 mg protein) was added to the beads and the volume brought to 400 µL with ice-cold PBS. The tube containing the beads was rotated end-over-end overnight at 4°C. The contents of the tube was centrifuged at 14,000 *g* for 5 s and the supernatant discarded. The beads were then transferred into a 15 mL conical tube using four 1-mL volumes of 200 mM sodium borate (adjusted to pH 9 with HCl) and then the beads were centrifuged at 2,500 *g* for 4 min at 22°C. The beads were washed with 4 mL of 200 mM sodium borate, then centrifuged as above. 10 µL of beads ('pre-coupling') were removed (see below). The remaining beads were resuspended in 4 mL of 200 mM sodium borate and the resuspension checked to ensure it did not shift from pH 9.0. Dimethylpimelimidate was added to yield a final molar concentration of 20 mM and dissolved. The pH was checked again to verify that it remained at 9.0 and then the mixture was incubated by rotating end-over-end for 30 min at 22°C. Following centrifugation at 2500 *g* for 4 min, the supernatant was discarded and 10 µL of beads ('post-coupling') were removed. The remaining beads were washed by resuspension with 4 mL of 200 mM ethanolamine (adjusted to pH 8.0 with NaOH) and centrifuged as above. The pelleted beads were incubated and rotated end-over-end with 4 mL of 200 mM ethanolamine for 2 h at 22°C. The ethanolamine was discarded and then the beads were washed twice with 4 mL PBS each time. The beads were finally resuspended with PBS resulting in a 1:1 suspension of beads in PBS. Na-azide was added to a final concentration of

0.1% (w/v) and the immuno-activated beads were stored at 4°C (Harlow and Lane, 1988).

To determine if the coupling was successful, the 'pre-coupling' and 'post-coupling' bead samples were mixed with solubilizing buffer, heated to 90°C for 3 min and the beads were pelleted by centrifugation. The supernatants were removed and subjected to SDS-PAGE. A successful coupling of the antibody to the beads was indicated by the presence of immunoglobulin proteins at approximately 55,000 Da in the 'pre-coupling' lane and no comparable band in the 'post-coupling' lane (Appendix 2).

Immunoprecipitation of PEAMT protein

PEAMT was purified from crude leaf extracts using the activated protein A agarose beads prepared as described above. Crude leaf extract (equivalent to 80 μg protein) were added to 70 μL antibody-protein A agarose bead suspension and the final volume raised to 200 μL with PBS. This mixture was incubated overnight at 4°C with end-over-end rotation. The tube was then centrifuged at 14,000 *g* for 5 s at 4°C and the supernatant removed and saved for analysis. The beads were washed with 1 mL of buffer containing 150 mM sodium chloride, 50 mM Tris-HCl pH 7.5, 1% (v/v) Nonidet P-40 or 1% (v/v) IGEPAL CA-630 ((octylphenoxy)polyethoxyethanol; Cat. No. I-3021, Sigma) and 0.5% (w/v) sodium deoxycholate for 20 min at 4°C with continuous end-over-end rotation. The suspension was centrifuged at 14,000 *g* for 5 s and the supernatant discarded. This wash was repeated twice. Beads were then washed two times with 1 mL buffer containing 500 mM NaCl, 50 mM Tris-HCl pH 7.5, 0.1% (v/v) Nonidet P-40 or 0.1% (v/v) IGEPAL CA-630 and 0.05% (w/v)

sodium deoxycholate. A final wash of the beads was done with 1 mL buffer containing 50 mM Tris-HCl pH 7.5, 0.1% (v/v) nonidet P-40 or IGEPAL CA-630 and 0.05% (w/v) sodium deoxycholate (Harlow and Lane, 1988). Residual supernatant was carefully removed and 30 µL of SDS-solubilizing buffer were added. The contents could either be subjected to SDS-PAGE and immunoblot analysis immediately or stored at -20°C for subsequent analysis.

Immunoblot analysis of PEAMT protein

Immunoaffinity purified PEAMT protein was released from the Protein A agarose suspended in SDS-PAGE solubilizing buffer by heating the beads at 90°C for 3 min. These samples were subjected to electrophoresis on a 7.5-15% gradient SDS-PAGE and then the polypeptides on the gels were transferred to nitrocellulose or Hybond™- P PVDF membranes (Cat. No. RPN303F Amersham-Pharmacia) overnight at 15 V in a Bio-Rad wet transfer apparatus (Trans-blot, Bio-Rad). After transfer, the membranes were stained with 0.2% (v/v) Ponceau S to visualize the polypeptides transferred to the membrane (Harlow and Lane, 1988). A photograph was taken to serve as a record of a successful transfer and to verify that equal loading of protein was achieved. Equal loading was judged by the size and intensity of the band corresponding to the large subunit of ribulose 1,5 bisphosphate carboxylase/oxygenase as its abundance was not expected to vary with any of the treatments used. PVDF membranes were then blocked for 1 h with 100 mL 1% (w/v) BSA in TBS, the membrane was rinsed with antibody dilution buffer and then the membrane was placed inside a seal-a-meal bag (Rossi, purchased from Canadian Tire) containing antisera to PEAMT

diluted 2,000-fold with antibody dilution buffer. All bubbles were removed and the bags were heat-sealed. Membranes were hybridized with the diluted primary antibody for 2 h with gentle shaking and then washed in a small Pyrex dish three times with 200 mL TTBS and once with 200 mL TBS for 15 min each wash. The second hybridization using 3,000-fold diluted goat anti-rabbit IgG (Cat. No. 170-6518, Bio-Rad) antibody was done as described for the primary antibody and the membrane washed three times with 200 mL TTBS and one time with 200 mL TTBS + 0.05% (w/v) SDS for 15 min each wash. Polypeptides hybridizing to the antibodies prepared against PEAMT were visualized in the colour development solution when the dark purple products of the alkaline phosphate/BCIP/ NBT reaction appear after several minutes (Sambrook *et al.*, 1989). To stop the reaction, the membrane was washed thoroughly with water and then it was left overnight in 0.05% (w/v) sodium azide. Blots were then air dried before imaging analysis.

ISOLATION AND NORTHERN BLOT ANALYSIS OF TOTAL RNA

In these procedures precautions were taken to minimize degradation of RNA by RNases. H_2O and all buffers used were made RNase-free by treatment with dimethyl pyrocarbonate (DMP; Cat. No. D-5520, Sigma). DMP was added to a final concentration of 0.05% (v/v), the solution swirled to mix and allowed to stand for 1 h before autoclaving. The electrophoresis apparatus were made RNase-free by soaking in 0.1% (v/v) DMP for 20 min and then rinsed with DMP-treated autoclaved H_2O. Liquid handling tips, microfuge tubes, mortars and pestles were autoclaved to sterilize before use.

Samples of leaf tissue previously frozen in liquid nitrogen and stored at -80°C were kept frozen in liquid nitrogen as they were ground in a mortar with a pestle to a fine powder. The powder was transferred to a tube containing 1 mL TRIzol® Reagent (Cat. No.15596-018, Invitrogen) per 100 mg tissue and swirled to mix. Insoluble material was removed by centrifugation at 12,000 *g* for 10 min at 4°C. The supernatant was transferred to a new tube and the pellet discarded. RNA was then purified by adding 200 µl chloroform per mL TRIzol reagent used followed by vigorous shaking and centrifugation at 12,000 *g* for 15 min at 4°C to separate the two phases. The upper, aqueous phase was transferred to a new tube to which 0.5 vol of isopropanol were added and the solution allowed to sit for 15 min at room temperature to precipitate the RNA. The RNA was pelleted by centrifugation at 12,000 *g* for 10 min at 4°C and the supernatant was discarded. The pellet was resuspended and washed with 0.2 vol of 75% (v/v) ethanol, then centrifuged at 7,500 *g* for 5 min at 4°C and the supernatant discarded. The RNA pellet was then air dried and dissolved with 200 µL sterile, RNase-free water. As the RNA preparations were found to contain traces of DNA and showed a low OD_{260} / OD_{280} ratio (see below), the samples of RNA were routinely re-extracted with 1 mL of TRIzol and subsequent steps were modified to include three additional phase separations with chloroform to remove any contaminants. The final RNA pellet was dissolved in 20 µL of sterile RNase-free water. Total RNA was quantified at 260 nm (1 OD_{260} = 40 µg mL^{-1} RNA) and quality was assessed by determining the OD_{260} / OD_{280} ratio. This ratio always exceeded 1.8, an indication that the RNA was of high quality (Maniatis *et al.*,

1982) (Appendix 3). Samples of total RNA were separated by electrophoresis on non-denaturing 1.5% (w/v) agarose gels containing 0.05 μg mL^{-1} ethidium bromide as described earlier for DNA. These gels were photographed to provide a record that RNA concentrations were determined accurately and RNA was loaded equally.

Total RNA (20 μg per lane) was separated on a 1.5% (w/v) agarose-formaldehyde gel in a Bio-Rad Sub apparatus (Sub-Cell Model 192 Cell, Bio-Rad) at 100 V for 3 h (Weretilnyk and Hanson, 1990). RNA was then transferred to a Hybond^{TM}-N^{+} nylon membrane (Cat. No.RPN203B, Amersham-Pharmacia) by a wet transfer method as described by Maniatis *et al.* (1982). The RNA was transferred from the gel onto the membrane with 20x SSC (0.3 M sodium citrate and 3.0 M NaCl) under capillary action overnight. Following transfer, membranes were washed of excess salt by rinsing three times for 5 min each time with 80 mL of 5 x SSC. The membrane was then prehybridized for 3 h in a buffer containing 5 x SSC, 10 x Denhardt's Solution (1% (w/v) Ficoll PM 400 (Cat. No. 17-0310-10, Amersham-Pharmacia), 1% (w/v) polyvinylpyrrolidone, 1% (w/v) BSA), 0.1% (w/v) SDS, 50 mM sodium phosphate pH 7, 100 μg mL^{-1} tRNA from brewer's yeast (Cat. No. 109 495, Roche Diagnostics) (Maniatis *et al.*, 1982) and then hybridized at 65°C in buffer containing 5 x SSC, 10 x Denhardt's Solution, 0.1% (w/v) SDS, 50 mM sodium phosphate pH 7, 10 μg mL^{-1} tRNA (Maniatis *et al.*, 1982) and a ^{32}P-labelled cDNA probe. The probe was obtained by random priming of PCR-amplified and gel-purified *peamt* cDNA insert. Gel purification of *peamt* insert was done using the QIAEX II Gel Extraction Kit for DNA extraction from

agarose gels (Cat. No. 20051, Qiagen, Chatsworth, California) following the manufacturer's directions. Random priming of the insert was done by denaturing 25 to 200 ng DNA dissolved in 6 μL H_2O by heating the DNA solution for 5 min at 95°C. To prevent reannealing, the DNA was then placed on ice for 5 min. Then dATP, dGTP and dTTP (Invitrogen) were added to a final concentration 66 μM each (Invitrogen), as well as 7 μL of 9.3 $A_{260}\,mL^{-1}$ $d(NTP)_6$ random primers, 2 μL large fragment of DNA polymerase (100 U, Cat. No. 18012-021, Invitrogen) and 4 μL ^{32}P-dCTP (NEN™ Life Science Products). This mixture was incubated at room temperature for 2 h. 80 μL of sterile H_2O were added and then 1 μL of the diluted mixture was removed and applied to a DE81 filter disk (Whatman Int. Ltd., Maidstone, England). The remainder was applied to a Sephadex G-50 (Amersham-Pharmacia) spin column equilibrated in STE buffer (0.1 M NaCl, 10 mM Tris-HCl pH 8, 1 mM EDTA; Sambrook *et al.*, 1989) and the column centrifuged in a clinical centrifuge at step 4 for 6 min. 1 μL of the eluate obtained by centrifugation was applied to a DE81 filter disk, air dried and placed in a liquid scintillation vial with 10 mL of fluor for liquid scintillation counting to determine incorporation of ^{32}P label and the remainder was denatured by adding 2 μL of 5 N NaOH per 25 μL of probe and incubated at room temperature for 5 min. The probe was then added to the hybridization buffer (Maniatis *et al.*, 1982) and the mixture added to the blot in a seal-a-meal bag for hybridization overnight at 60°C. Hybridized membranes were washed to a final stringency of two 15 min washes at 65°C in 0.1 x SSC, 0.1% (w/v) SDS. Probe hybridizing to RNA on the membrane was revealed by autoradiography on Kodak Scientific

Imaging film (X-OMAT, Cat. No.165 1454, Eastman Kodak Company, Rochester, New York). Equal loading of total RNA from preparations used for Northern blot analysis was shown by photographing ethidium bromide stained non-denaturing 1.5% (w/v) agarose gels.

QUANTIFICATION OF WESTERN AND NORTHERN BLOTS

Blots were photographed using the Kodak ImageStation 440CF System and images analysed using Kodak 1D Image Analysis Software (Eastman Kodak Company). In all cases, data was normalized to the band intensity given by the sample at time 0 h or the relevant control sample.

RESULTS

Polyclonal Antibodies raised against PEAMT

One aspect of the study undertaken involved quantifying PEAMT protein levels in spinach leaves using western blot hybridization analysis. The polyclonal antibodies were generated using a recombinant polyhistidine-tagged PEAMT protein as antigen. For subcloning, the DNA sequence of the spinach cDNA encoding PEAMT was first modified to introduce the restriction sites *Nco* I and *Bam*H I (Appendix 1a). These restriction sites were chosen since they are absent from the *peamt* sequence and so these enzymes would not restrict the coding sequence and an *Nco* I restriction site is a convenient way to position a translation initiation site for the pET30a (+) vector (pET System Manual, Novagen). The oligonucleotide primers used for PCR were designed to incorporate the desired restriction sites and would eliminate a large portion of 3' non-coding sequence leading to an insert of 1.5 Kb.

In order to verify that the DNA fragment subcloned into pET30a (+) was correct, plasmid preparations from transformed DH5α cells were digested by *Nco* I and *Bam*H I and the resulting DNA fragments separated by electrophoresis. Figure 3 shows the migration of two bands on the gel: the 6.08 Kb DNA fragment corresponds to the size of the pET30a (+) vector and the smaller 1.54 Kb DNA fragment corresponds to the estimated size for the

FIGURE 3: Gel electrophoresis analysis of restriction digested and PCR amplified plasmid carrying cDNA insert encoding PEAMT

In panel A, *peamt* subcloned into pET30a (+) was used to transform DH5α and transformant bacteria were used to isolate plasmids. These plasmids were digested with *Nco* I and *Bam*H I. The arrows denote the positions of 6.08 Kb and 1.54 Kb fragments corresponding to pET30a (+) vector DNA and the *peamt* cDNA insert, respectively. Panel B shows the position of the 1.54 Kb DNA fragment corresponding to the *peamt* cDNA insert amplified by PCR. Reaction products were separated electrophoretically by loading 6 μL onto a non-denaturing 1.2% agarose gel containing ethidium bromide (see Materials and Methods). The DNA was visualized by illumination with UV light. Position of MW standards is given.

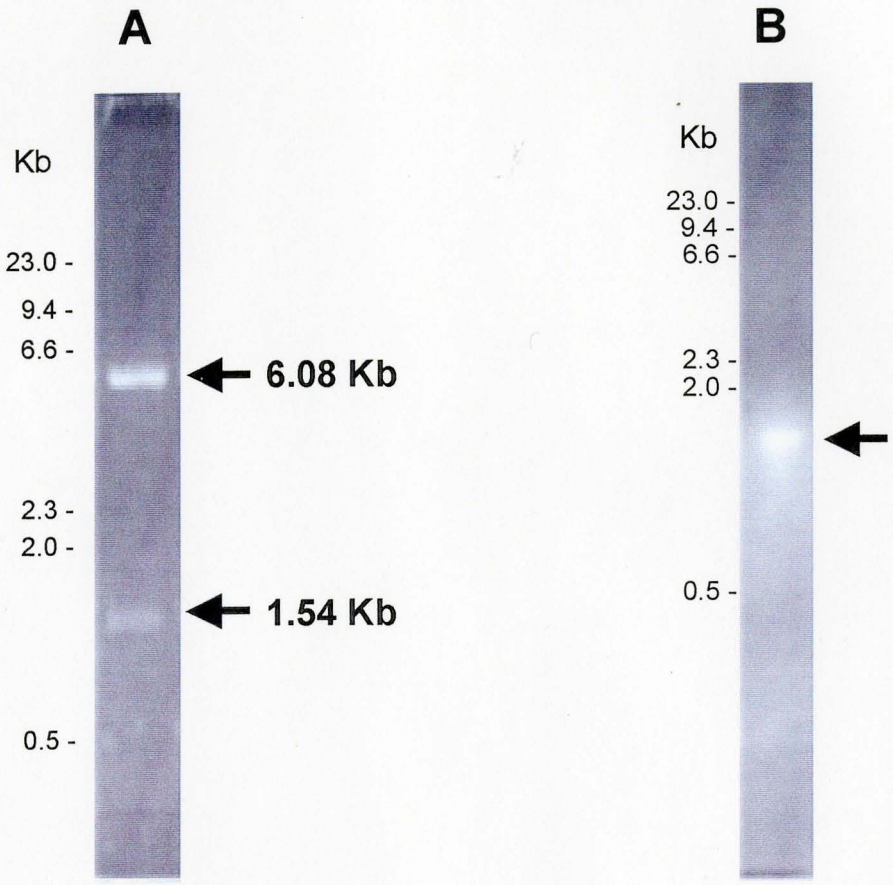
A
Kb
23.0 -
9.4 -
6.6 -
2.3 -
2.0 -
0.5 -
6.08 Kb
1.54 Kb
B
Kb
23.0 -
9.4 -
6.6 -
2.3 -
2.0 -
0.5 -

modified *peamt* cDNA insert. The same plasmids were subjected to PCR and the only DNA fragment amplified was also 1.5 Kb in size. DNA sequence analysis confirmed the identity of the insert and verified that the desired changes had modified the 3' and 5' ends of the original *peamt* cDNA. This plasmid preparation was used to transform the expression host BL21(DE3) and successful transformants were identified and verified in the same manner as the DH5α transformants described above (data not shown). Expression of a recombinant protein was induced in BL21(DE3) transformants containing the *peamt*-vector construct and PEAMT enzyme activity was detected in cell-free extracts of the bacteria. Extracts prepared from BL21(DE3) containing the *peamt* cDNA-vector construct showed enzyme activities of 216.8 ± 41 nmol mg^{-1} protein min^{-1}, whereas extracts prepared from bacteria with plasmids lacking a *peamt* cDNA insert showed no PEAMT activity. Figure 4 shows an SDS-PAGE gel separating proteins from a cell-free extract of BL21(DE3) induced to overexpress the recombinant protein and shows a predominant polypeptide with a molecular mass (Mr) of 59.5 kDa among the polypeptides present in the bacterial cell-free lysate. This polypeptide band corresponds to the molecular mass of the polyhistidine-tagged PEAMT protein and is denoted by the solid arrow in Figure 4. Four independent affinity column protein separations of the crude, cell free extract were performed to purify polyhistidine-tagged PEAMT. A maximum of 17 mg total protein was loaded onto each 1-mL metal affinity column but only approximately 8% total protein loaded was recovered in fractions 2 to 4 of nine fractions collected. Figure 4 shows that the prominent polypeptide eluting from the column has a Mr

FIGURE 4: SDS-PAGE analysis of recombinant PEAMT purified by chromatography on a metal affinity resin

Cell free extract of BL21(DE3) transformed with a plasmid induced to express recombinant PEAMT was subjected to chromatography on a cobalt metal affinity column. Polypeptides loaded on the column and eluting from the matrix were separated by electrophoresis on a 7.5-15% SDS-polyacrylamide gel and the gel stained with silver reagent. Protein equivalent to 1.5 μg and 2.0 μg were applied to the gel for the load and fractions, respectively. Specific activity associated with the load and fractions are given below the lane. The arrow on the right denotes the position of the 59.5 kDa polypeptide corresponding to the polyhistidine-tagged recombinant PEAMT protein.

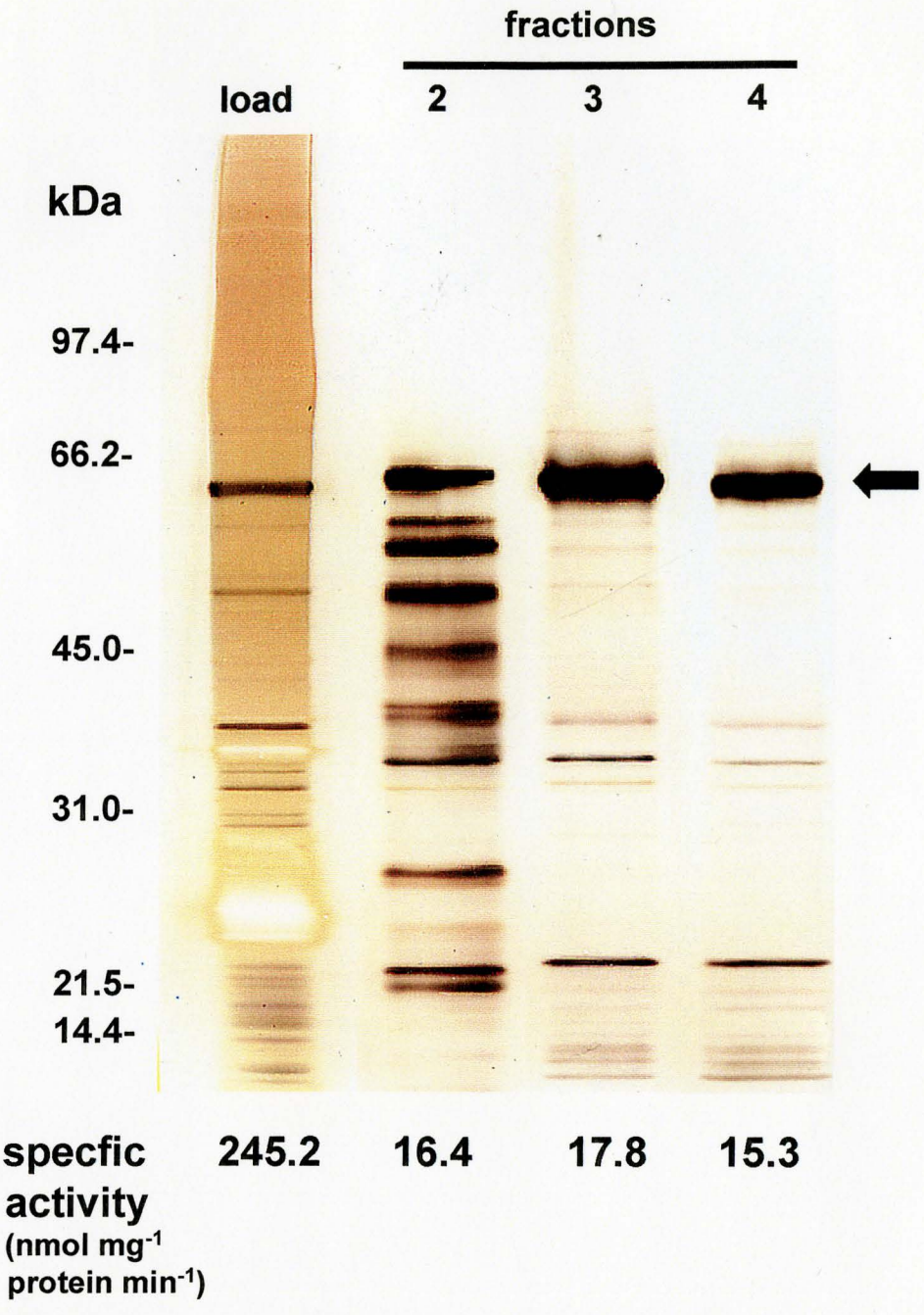
fractions
load
2
3
4
kDa
97.4-
66.2-
45.0-
31.0-
21.5-
14.4-
specfic activity (nmol mg-1 protein min-1)
245.2
16.4
17.8
15.3

of 59.5 kDa. Of the fractions collected, the second one has considerably fewer contaminating proteins than the load but was less pure than fractions 3 and 4. Fractions 3 and 4 were enriched with respect to PEAMT protein abundance and showed a different and less complex profile relative to fraction 2. SDS-PAGE analysis of similar fractions from other columns showed recombinant PEAMT preparations of comparable purity. Since PEAMT was the predominant polypetide, fractions exemplified by Nos. 3 and 4 were used to prepare the protein antigen for immunization to generate polyclonal antibodies. Fractions were assayed for PEAMT activity and negligible activity was found relative to that detected in the sample loaded. The fractions with recombinant PEAMT contained comparable levels of activity (17.1 $\pm$ 4.3 nmol mg^{-1} protein min^{-1}), a level that is almost 13-fold lower than in the load. The cause of this decrease in PEAMT activity after elution from the metal affinity column is unknown. The buffers and reagents used in the purification did not inhibit PEAMT activity when added to *in vitro* enzyme activity assays discounting detrimental effects due to the extraction/wash buffer, extraction/wash buffer + β-mercaptoethanol, and elution buffer (for components see Materials and Methods). Thus, the cause of the decrease in PEAMT activity in fractions from the column relative to the cell-free extract loaded onto the column is unknown.

The serum collected at each bleed was analysed for antibody titre. In order to determine titre, dot blot immunoassays were conducted for the preimmune serum and each antisera collected with all tested at a dilution of 1,000-fold (see Materials and Methods). Figure 5 shows the immunoblot analysis of the preimmune serum with no cross-reaction with

FIGURE 5: Dot blot immunoassay analysis of serum taken pre and post immunization with recombinant PEAMT

Various quantities of antigen were applied to individual spots on a nitrocellulose membrane. Antigen was applied as non-denatured ('native') and SDS-denatured protein. Serum from each collection made post-immunization from the earliest (1) to final (4) was diluted 1000-fold for hybridization detection tests. Time of post-immunization collections were at 2, 6, 8 and 10 weeks following the booster injection for serum samples 1 to 4, respectively. Conditions of the antigen preparation and immunodetection procedures are described in the Materials and Methods. The intensity of the blue colouration is indicative of a stronger cross-reaction between the antibody preparation and the antigen.

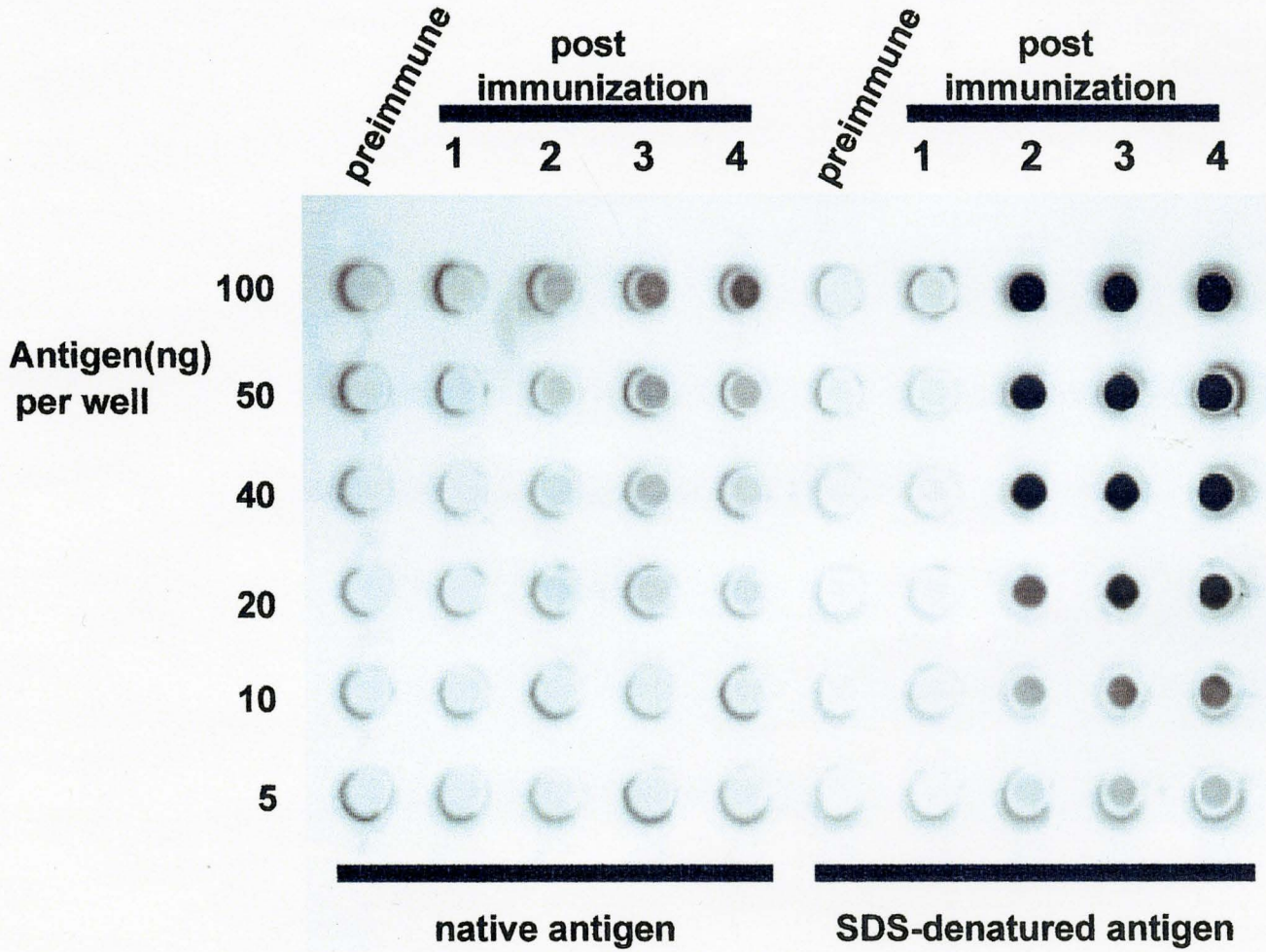
preimmune
post immunization
1 2 3 4
preimmune
post immunization
1 2 3 4
Antigen(ng) per well
100
50
40
20
10
5
native antigen
SDS-denatured antigen

native or denatured antigen. Indeed, diluted antisera from the first post-immunization serum can detect a level of 100 ng native or denatured antigen and the level of immunodetection improves after the first booster with detection limits of 20 ng native and 5 ng (the lowest level tested) denatured recombinant PEAMT, respectively. Subsequent serum recoveries show the highest cross-reaction with the antigen; both detect 10 ng of native and 5 ng denatured recombinant PEAMT (Fig. 5).

Antibody specificity and use in immunoblot hybridization analysis

Antibody specificity was determined by western blot hybridizations comparing the immuno-specificity of preimmune serum with that of the serum collected with the highest titre (antiserum obtained following the second collection). Figure 6 shows that polyclonal antibodies cross-reacted with the PEAMT antigen in the soluble extract prepared from *E. coli* induced to overexpress the fusion protein and in a sample of protein obtained following chromatography on the metal affinity matrix (see Materials and Methods for details) with a 2,000-fold dilution. Comparably diluted preimmune serum did not cross-react with any polypeptides present in these lanes. For spinach, cross-reaction of the antisera with polypeptides present in crude leaf extracts from unsalinized and salinized plants was also seen, one of Mr 15 kDa was also detected by preimmune serum (Fig 6). The non-recombinant PEAMT protein migrates to a different position on the gel than the recombinant PEAMT protein since it does not have a polyhistidine-tag at its N-terminus. PEAMT present in spinach has a Mr of 56.4 kDa (Nuccio *et al.*, 2000). However, Figure 6 also shows that

FIGURE 6: Western blot hybridization analysis of recombinant PEAMT over-expressed by BL21 (DE3) and PEAMT from extracts of spinach leaves

Crude, cell free extract of BL21 (DE3) induced to express *peamt* (10 μg protein), partially purified PEAMT preparation (2 μg protein), control spinach leaf extract (50 μg protein) and 200 mM salinized spinach leaf extract (50 μg protein) were loaded two times on two identical halves of one SDS-PAGE gel. The proteins on the gel were transferred electrophoretically to a nitrocellulose membrane which was cut in half. The left portion was subjected to Western analysis by 1000-fold diluted preimmune serum and the right portion was subjected to Western analysis by 1000-fold diluted immune serum. The conditions of SDS-PAGE gel electrophoresis and Western blot hybridization analysis were as reported in the Materials and Methods. The square bracket along the right side of the gel denotes the diffuse band of the 54 kDa PEAMT protein from crude extract. Arrows along the right side of the gel denote the positions of the 59.5 kDa polyhistidine-tagged PEAMT protein and an unidentified polypeptide at approximately 53 kDa.

Immune
Preimmune
E. coli
Spinach
Cell-free Extract
Affinity-Purified
Control
200 mM Salt

several polypeptides cross-reacted with the anti-PEAMT antibodies and that the reaction expected at the position of spinach PEAMT (denoted by a square bracket in Fig 6) produced a more diffuse signal in the samples from spinach as compared to those from recombinant PEAMT induced in BL21(DE3). The polypeptide immunodetected in spinach extracts was approximately 53 kDa in size.

The diffuse nature of the signal associated with spinach PEAMT is a consequence of the presence of a far more abundant polypeptide co-migrating to the same position on the gel. The LSU of Rubisco also has a 55 kDa Mr and since Rubisco comprises at least 50% of the total soluble leaf protein (Raven *et al.*, 1999), its presence essentially displaces PEAMT and greatly diminishes the signal arising from immuno-reaction with anti-PEAMT antibodies. To mitigate this problem we immunoaffinity purified PEAMT from crude leaf extracts using protein A agarose beads to which PEAMT antibody has been coupled (see Materials and Methods for details). Figure 7 shows representative immunoblots comparing the crude extract from spinach leaves with extract subjected to immunoaffinity purification before analysis. In each case the amount of protein in the crude sample used was identical. All the PEAMT protein within the extract was bound to the activated Protein A agarose beads during the affinity purification procedure since no PEAMT could be detected in an aliquot of the supernatant representing protein not bound to the beads. A distinct band corresponding to PEAMT is detected in the affinity purified protein sample, the intensity of this band can be quantified using the Kodak image system to provide an estimate of the relative PEAMT

FIGURE 7: Western blot hybridization analysis of spinach leaf extracts subjected to immunoaffinity purification

A representative crude extract of spinach leaf was analysed directly on a 7.5-15% SDS-polyacrylamide gel. A similar sample containing 80 μg protein was immunoaffinity purified prior to electrophoresis. Also tested was an aliquot of the supernatant obtained after the first binding step, a sample carrying all proteins not bound to the activated beads. Conditions of immunoaffinity purification, electrophoresis and immunoblot analysis are described in the Materials and Methods.

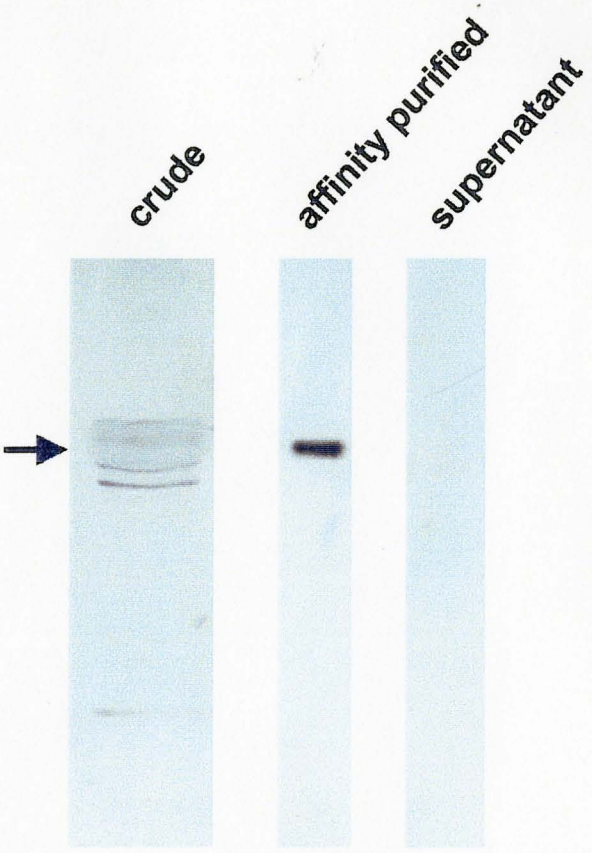
crude
affinity purified
supernatant

protein level in the sample. By comparison, the signal associated with the crude unpurified sample is more diffuse, a signal that cannot be easily quantified by the Kodak imaging software.

Regulation of PEAMT Activity by light

PEAMT specific activity, protein and transcript levels were examined in extracts of leaves harvested from plants placed under differing conditions of light. To characterize the light regulation of spinach PEAMT, plants were exposed to 60 h continuous light after a normal (16 h) night cycle. Harvesting of plant leaf tissue began during the night cycle and continued at 4 - h intervals for 72 h. Changes in the specific activity of PEAMT over the course of the experiment is shown in Figure 8. As reported by Weretilnyk *et al.* (1995), PEAMT activity decreases during the dark period and increases almost 12-fold over 24 h relative to the activity from plants harvested when the lights are turned on (time = 0 h). PEAMT activity in the light remains relatively constant over the next 56 h. However, a slight decrease at about 40 and 60 h post-illumination was shown for the results of two, independent repeats of this experiment. The standard error bars indicate that there was variability in absolute rates of PEAMT activity measured between plants but this could not explain the decrease in enzyme activity noted at 40 and 60 h.

Western blot hybridization analysis of these plant leaf extracts shows changes in protein levels with a decrease during the initial dark period and increases after the lights are turned on (Fig. 9). When estimates of the fold-changes are made using the Kodak imaging

FIGURE 8: Changes in PEAMT specific activity with exposure to continuous light

Plants were exposed to 60 h continuous light after being grown for 5 weeks under an 8 h light/ 16 h dark photoperiod. The extracts were prepared from leaves harvested at 4 - h intervals over the experimental period and used to assay for PEAMT activity and protein concentration (see Materials and Methods). PEAMT specific activity over time (h) is shown with each point corresponding to the average ± standard error of at least four measurements for two independent repeats of this experiment. The arrow denotes time = 0 h when lights were turned on. The bar below the graph denotes the subjective light (□) and dark (▒) periods (upper half) and the actual light (□) and dark (■) treatment conditions (lower half).

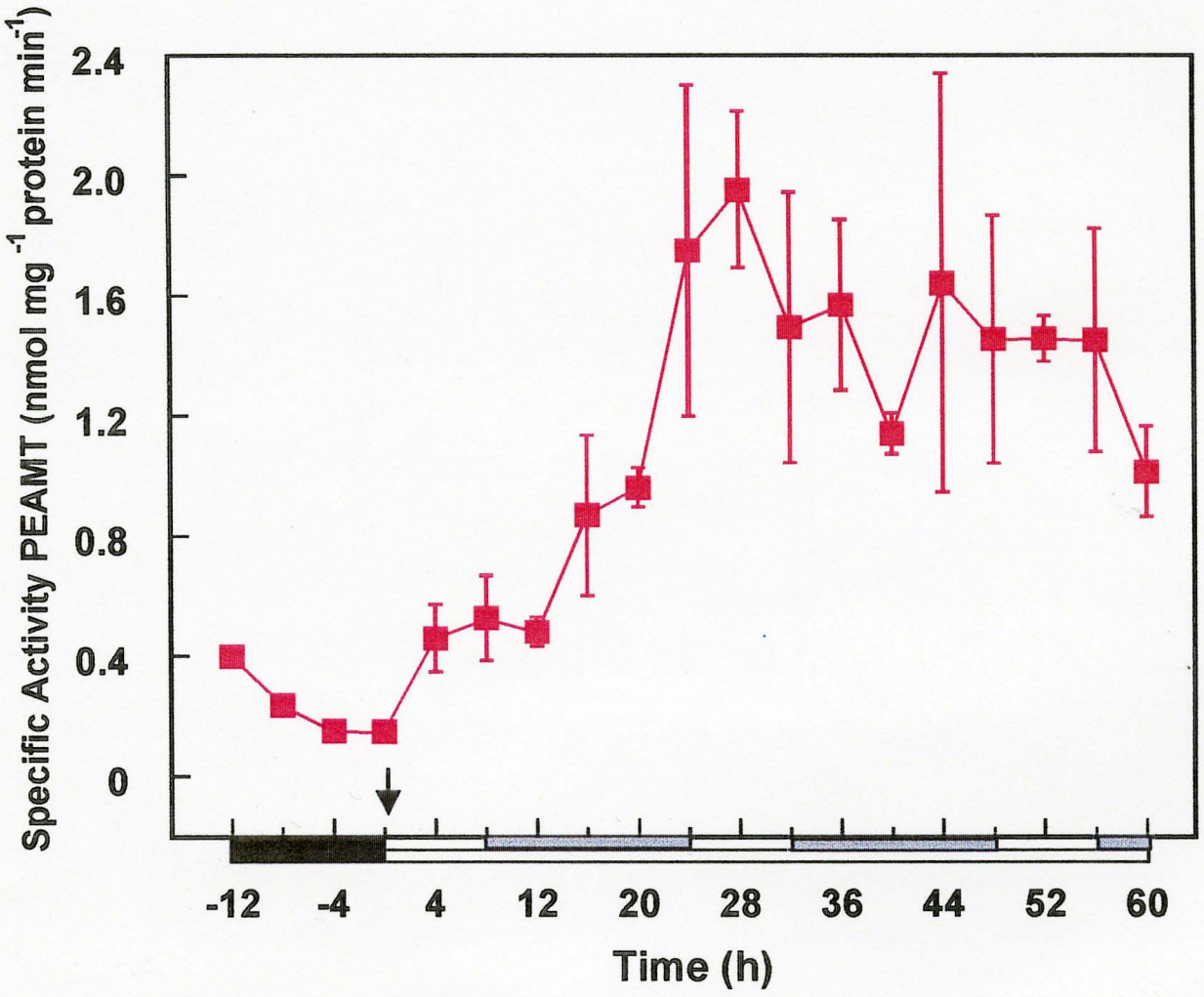
Specific Activity PEAMT (nmol mg -1 protein min-1)
2.4
2.0
1.6
1.2
0.8
0.4
0
-12
-4
4
12
20
28
36
44
52
60
Time (h)

FIGURE 9: Changes in PEAMT specific activity, protein and transcript levels with exposure to continuous light

Plants were exposed to 60 h continuous light after being grown for 5 weeks under an 8 h light / 16 h dark photoperiod. The extracts were prepared from leaves harvested at 4 - h intervals over the experimental period. Western blot and Northern blot hybridizations are shown in Panel A with appropriate loading controls shown immediately below. The conditions used for RNA isolation and quantification is described in the Materials and Methods. 1.5% agarose formaldehyde gels used for Northern blot hybridizations were loaded with 20 µg total RNA per lane. Equal loading was verified by comparing the intensity of the rRNA separated on a 1.5% agarose gel. For immunoblot analysis, 80 µg protein from crude leaf extracts was subjected to immunoaffinity purification followed by SDS-PAGE. To ensure that equal protein was used for immunopurification of each sample, the supernatant obtained in the first step of each immunopurification was also subjected to SDS-PAGE and transferred to membranes. In this case the membrane was stained with Ponceau S to reveal the LSU of Rubisco in each sample.

Panel B shows the estimated fold change of PEAMT activity (■), protein (●), and *peamt* transcript (▲) levels relative to time = 0 h. The solid arrow designates "lights on" at time = 0 h.

Changes in PEAMT Specific Acitvity, Protein and Transcript Levels with Exposure to Continuous Light

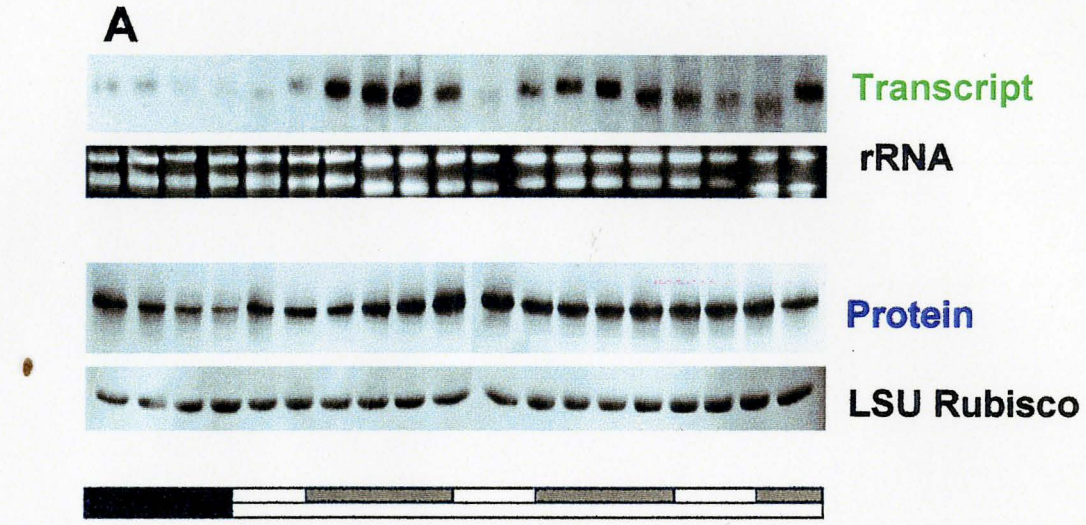

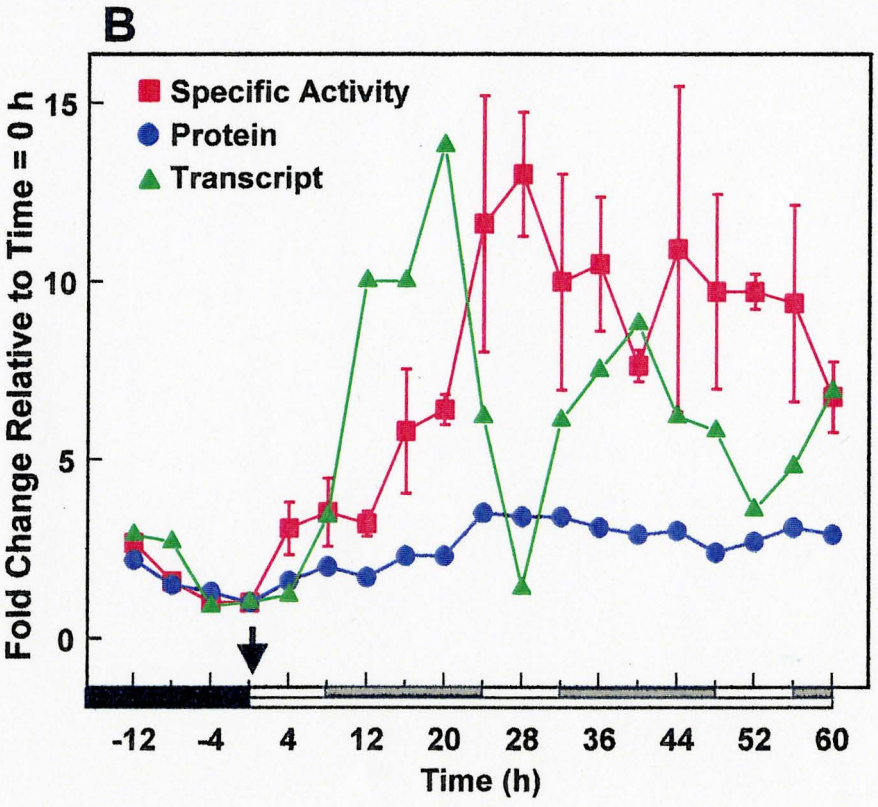

software, the increase over the 24 h light period results in an estimated 3.5-fold change in PEAMT protein level relative to time = 0 h. The protein level thereafter becomes relatively constant with an average fold change of 3.3. Thus the pattern of changes in PEAMT activity levels are associated with changes in PEAMT protein. The loading control for immunoblotting is shown under the PEAMT protein blot in Panel A and shows a relatively constant intensity for the LSU of Rubisco in each lane.

Changes in PEAMT transcript levels were evaluated by Northern blot hybridization analysis of total leaf RNA (Fig. 9, Panel A). Only a single band hybridizing to the radiolabelled probe appeared on the resulting autoradiographs. Relative band intensities estimated by the Kodak imaging software are shown graphically in Figure 9, Panel B. When the lights are turned on, transcript levels increase approximately 14-fold over a period of 20 h continuous light. Transcript accumulation peaks between 16 and 24 h and then decreases to levels at the threshold of detection between 24 and 32 h. Transcript levels then increase and peak again between 36 and 44 h and this is followed by another trough in transcript abundance between 48 and 56 h. The peaks in transcript levels correspond to the middle of the subjective dark periods and the troughs to the middle of the subjective light periods. These changes in *peamt* transcript levels do not coincide with changes in levels of PEAMT activity or protein (Fig. 9, Panel B). That is, when both PEAMT activity and protein levels are high and relatively constant under continuous light, *peamt* transcript levels undergo changes. These changes are circadian in that they are changes that persist in the absence of a day/night cue with levels

increasing during the subjective dark periods and decreasing during the subjective light periods.

Treatment of plants with a prolonged dark period was used to further characterize the regulation of PEAMT by light and to determine whether common patterns with the results of continuous light exposure would emerge. Plants were exposed to 60 h continuous darkness after a normal 8 h day. Plant leaf tissue for this treatment was harvested at the end of the normal light period (designated time = 0 h), again at 30 min, followed by 1- h intervals for 6 h and 4 - h intervals thereafter. *In vitro* PEAMT activity in the leaf extracts prepared from the harvested material is shown in Figure 10. PEAMT activity is high at the end of the normal light period (time = 0 h) and decreases over 10-fold during the course of the subsequent 24 h dark period to a basal level of activity of of 0.09 nmol mg^{-1} protein min^{-1} that remains relatively unchanged over the following 36 h. Western blot hybridization analysis of these plant leaf extracts shows that changes in PEAMT protein levels over time in the dark correspond well to changes in PEAMT activity (Fig. 11, Panel A). The relative intensities of these bands were determined using the Kodak Image System and are shown graphically in Figure 11 (Panel B). Thus PEAMT activity and protein levels (relative to time = 0 h) decrease almost 10-fold over the first 24 h of darkness and are low and relatively constant thereafter. The changes in PEAMT activity levels and PEAMT protein (Fig. 11, Panel B) yield lines that are superimposable. These results parallel those seen in the light experiment, in that changes in PEAMT activity and protein levels are positively correlated. Finally the loading control,

FIGURE 10: Changes in PEAMT specific activity with exposure to continuous dark

Plants were exposed to 60 h continuous dark after being grown for 5 weeks under an 8 h light/ 16 h dark photoperiod. The extracts were prepared from leaves harvested at the end of the normal light period (designated time = 0 h), again at 30 min, followed by 1 - h intervals for 6 h and 4 - h intervals thereafter and used to assay PEAMT activity and protein concentration (see Materials and Methods). PEAMT specific activity over time (h) is shown with each point corresponding to the average ± standard error of four measurements for two independent repeats of an experiment done over 12 h and two measurements for one experiment done over 60 h of darkness. The arrow denotes time = 0 h when lights were turned on. The bar below the graph denotes the subjective light (□) and dark (▒) periods (upper half) and the actual light (□) and dark (■) treatment conditions (lower half).

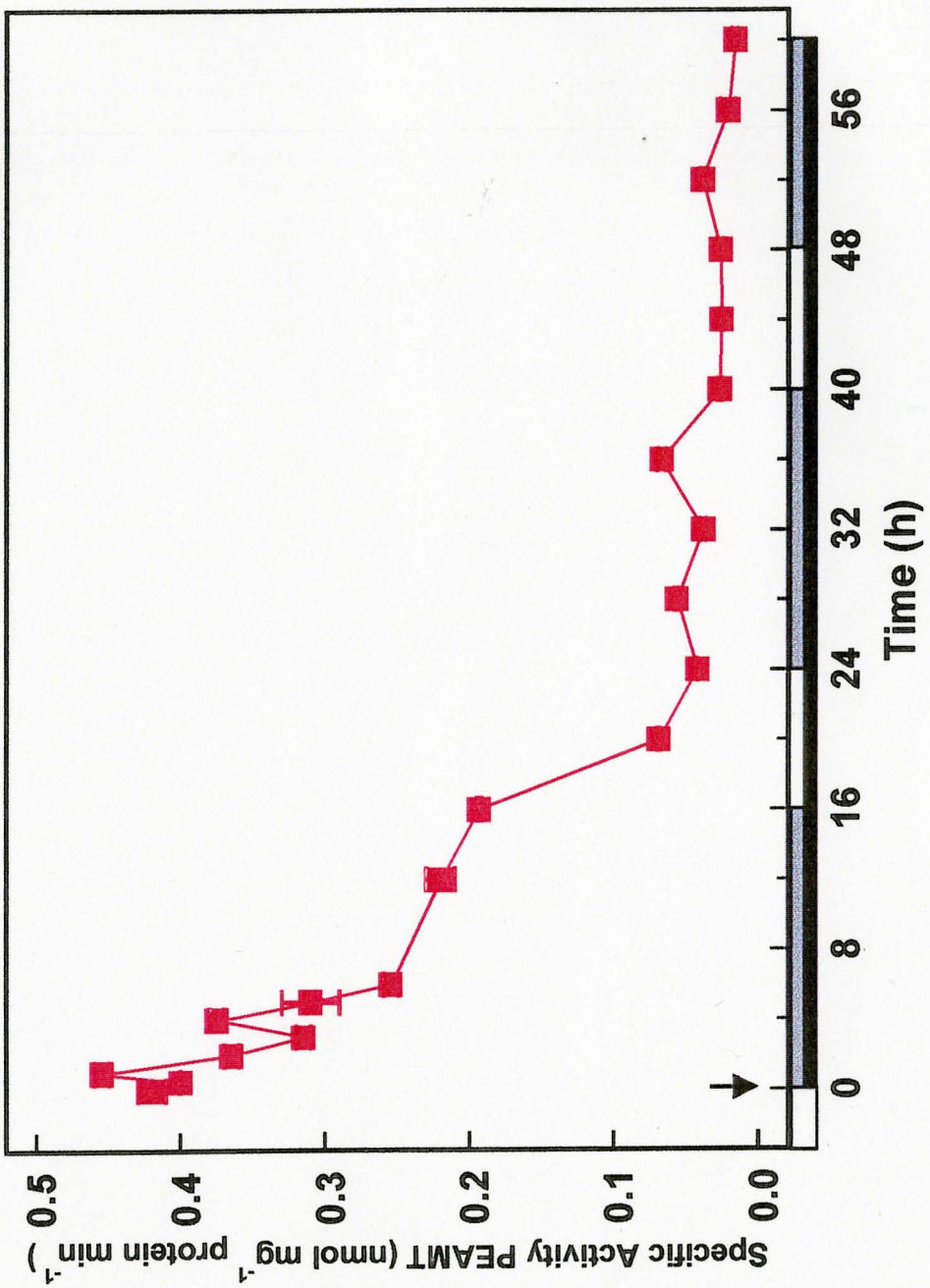
Specific Activity PEAMT (nmol mg-1 protein min-1)
0.0
0.1
0.2
0.3
0.4
0.5
0
8
16
24
32
40
48
56
Time (h)

FIGURE 11: Changes in PEAMT specific activity, protein and transcript levels with exposure to continuous dark

Plants were exposed to 60 h continuous dark after being grown for 5 under an 8 h light/ 16 h dark photoperiod. The extracts were prepared from leaves harvested at the end of the normal light period (designated time = 0 h), again at 30 min, followed by 1 - h intervals for 6 h and 4 - h intervals thereafter. Western blot and Northern blot hybridizations are shown in Panel A with appropriate loading controls for each shown immediately below. The conditions used for RNA isolation and quantification is described in the Materials and Methods. 1.5% agarose formaldehyde gels used for Northern blot hybridizations were loaded with 20 μg total RNA per lane. Equal loading was verified by comparing the intensity of the rRNA separated on a 1.5% agarose gel. For immunoblot analysis, 80 μg protein from crude leaf extracts was subjected to immunoaffinity purification followed by SDS-PAGE. To ensure that equal protein was used for immunopurification of each sample, the supernatant obtained in the first step of each immunopurification was also subjected to SDS-PAGE and transferred to membranes. In this case the membrane was stained with Ponceau S to reveal the LSU of Rubisco in each sample.

Panel B shows the estimated fold change of PEAMT activity (■), protein (●), and *peamt* transcript (▲) levels relative to time = 0 h. The solid arrow designates "lights on" at time = 0 h.

Changes in PEAMT Specific Activity, Protein and Transcript Levels With Exposure to Continuous Dark

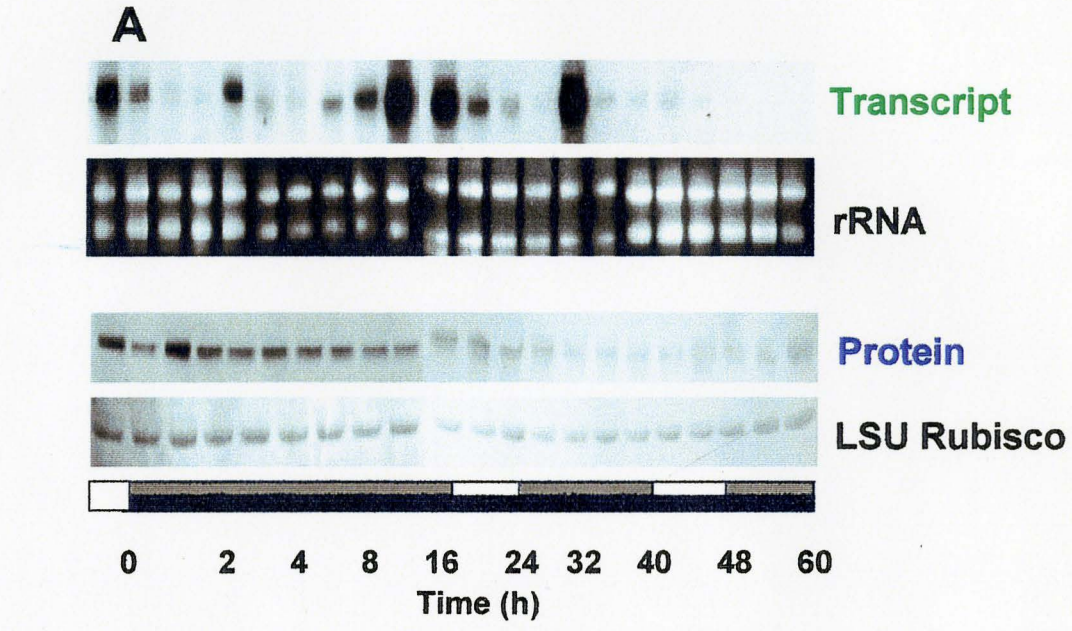

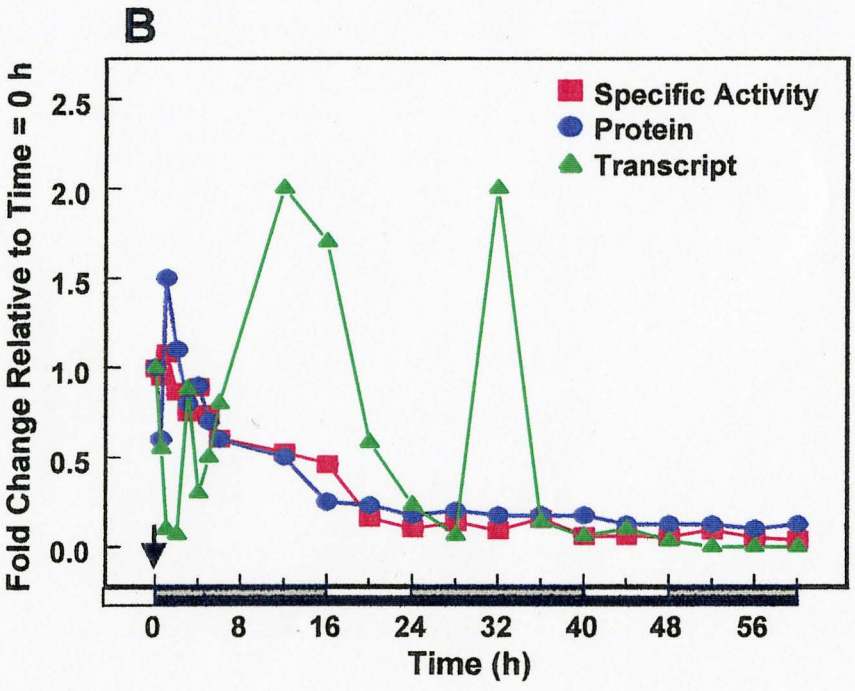

directly beneath the protein immunoblot, shows the equal intensity of the band corresponding to the LSU of Rubisco in each lane (Fig. 11, Panel A).

PEAMT transcript levels are also shown in Figure 11 (Panel A). The abundance of the single band found hybridizing to the radiolabelled probe was also quantified using the Kodak Image System. Estimated values of band intensities were made relative to transcript abundance at time = 0 h and are shown graphically in Figure 11 (Panel B). When the lights are turned off, *peamt* transcript levels increase over 12 h by 3-fold with a peak in abundance occurring between 6 and 16 h. This peak is followed by a decrease to transcript levels at the threshold of detection by Northern blot analysis reached after 26 h. Transcript levels then increase again to peak between 28 and 36 h of darkness and then decrease until levels became virtually undetectable. The peaks and troughs correspond to the middle of the subjective dark and subjective light periods, respectively. These results resemble those of the light experiment in that they show a cyclical nature that persists in the absence of changes in the environmental cue and as such, are circadian in nature. Moreover, the changes in *peamt* transcript levels are not associated with comparable changes in either PEAMT activity or protein levels. Thus when both PEAMT specific activity and protein levels remain low and relatively constant under conditions of continuous darkness, *peamt* transcript levels undergo increases during the first two subjective dark periods and decreases during the subjective light periods. However, no increase in transcript level is seen during the third subjective dark period (40 - 60 h period). These results show that the circadian rhythm diminishes after plants are

exposed to darkness in excess of 40 h.

Regulation of PEAMT by light and salinity

We sought to determine whether the salt-induced increase in PEAMT activity was associated with elevated transcripts and whether the pattern of circadian changes in transcript abundance would persist under salt-stress. For this study plants were either unsalinized (controls) or salinized to 200 mM NaCl under a normal diurnal cycle. Harvesting of control and salinized plant tissue for this treatment was initiated at the end of the normal (16 h) dark period and continued at 4 - h intervals for 16 h. Changes in PEAMT transcript levels were evaluated by Northern blot hybridization analysis of total RNA isolated from each of the harvested leaf samples. Figure 12, Panel A shows the changes in transcript levels associated with *peamt* over time both with and without salt treatment. Values for the band intensities relative to time = 0 were determined by the Kodak Image System, and shown graphically in Figure 12, Panel B. In the light, transcript levels for control and salinized plants decrease and at the onset of the dark period the transcript levels begin to increase again. These results resemble those seen in the continuous light and dark experiments. The band intensities shown for salinized plants, indicate that these plants have higher transcript levels than control plants but salinization does not appear to override the control by circadian oscillations of *peamt* transcript abundance in these plants.

FIGURE 12: Changes in PEAMT transcript levels with time and in response to salt

Leaf tissue from control (unstressed) and salt-stressed plants was harvested over 16 h of a normal 8 h day / 16 h night cycle. Tissue collection began at the end of the normal dark period and then at 4 - h intervals. The Northern blot hybridization is shown in Panel A. For this analysis a 1.5% (w/v) agarose formaldehyde gel was loaded with 20 µg total RNA per lane. The conditions used for transfer and hybridization are reported in the Materials and Methods. Equal loading was verified by separation of 4 µg total RNA loaded from these samples on 1.5% (w/v) agarose gels and detection of the rRNA.

Panel B shows the fold change *peamt* transcript levels relative to time = 0 h (denoted by the solid arrow) as quantified by the Kodak image software for control plants (■) and plants salinized to 200 mM NaCl (■). The entire experiment was repeated twice with comparable results each time.

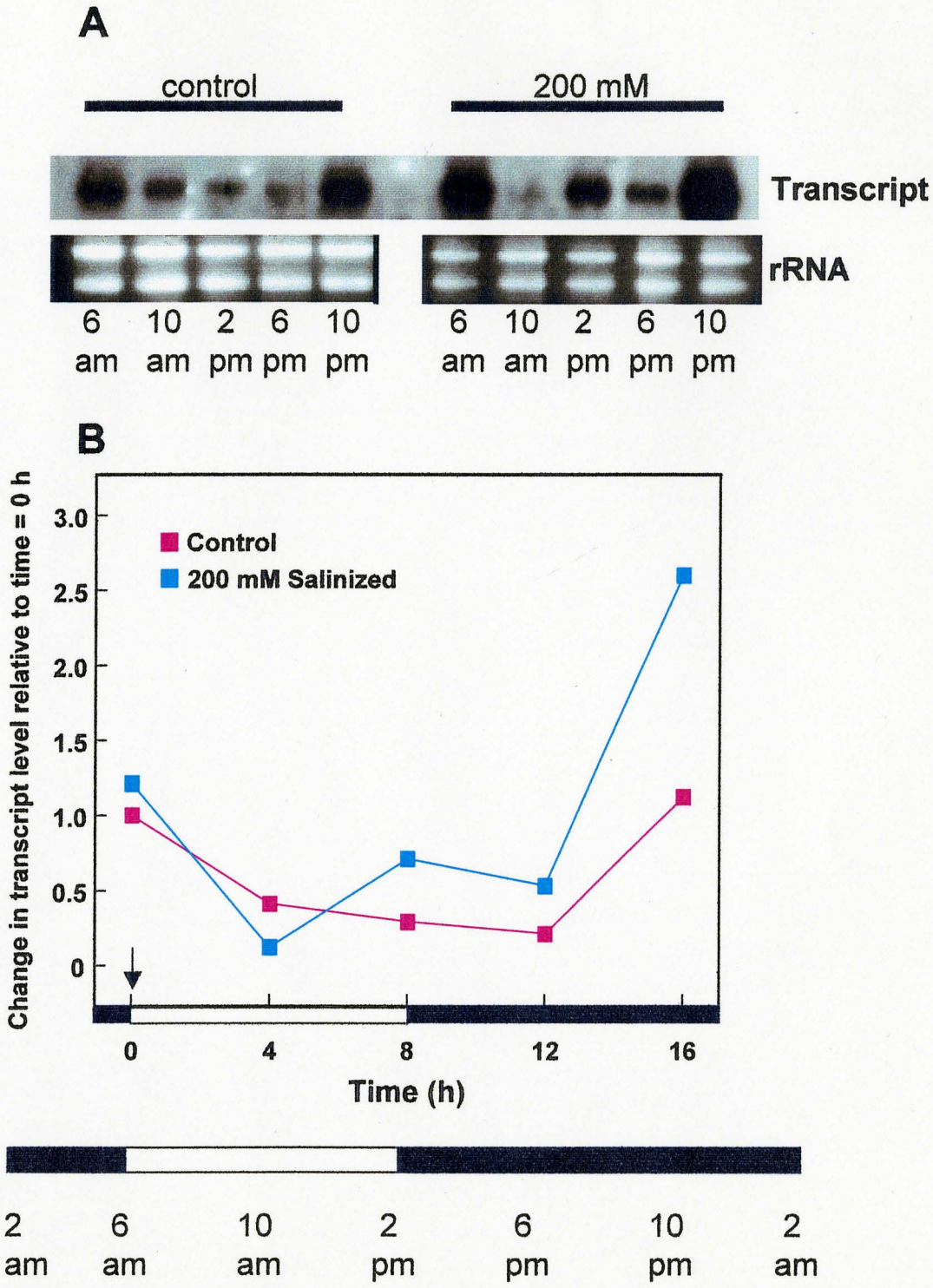
A
control
200 mM
Transcript
rRNA
6 am
10 am
2 pm
6 pm
10 pm
6 am
10 am
2 pm
6 pm
10 pm
B
Change in transcript level relative to time = 0 h
3.0
2.5
2.0
1.5
1.0
0.5
0
Control
200 mM Salinized
0
4
8
12
16
Time (h)
2 am
6 am
10 am
2 pm
6 pm
10 pm
2 am

DISCUSSION

PEAMT

The objective of this study was to characterize how PEAMT activity is regulated *in vivo*. PEAMT activity is both light and salt-responsive. In spinach leaves PEAMT activity increases when plants are exposed to light and when plants are salt-stressed (Smith *et al.*, 2000; Summers and Weretilnyk, 1993). As is true for any enzyme, changes in activity could reflect changes in protein activation state or abundance, gene expression or transcript abundance, or any combination of the preceding mechanisms. Preliminary work by Smith *et al.* (2000) has shown that the PEAMT protein levels in extracts from leaves of plants in the light are higher when they are salt-treated compared to unstressed control plants. Moreover, during the dark period PEAMT protein levels are low in both salt-treated and control plants. An examination of the changes in PEAMT activity, protein and *peamt* transcript levels in the leaves of spinach plants exposed to different light/dark regimes and in response to salt-stress was undertaken in this work.

The spinach *peamt* cDNA sequence was used for overexpression of the recombinant PEAMT protein in bacterial cells and for probing Northern blots loaded with total RNA. A sample of the recombinant PEAMT protein was used to generate polyclonal antibodies that were used to immunopreciptitate spinach PEAMT and for subsequent immunoblot

hybridizations.

Cell-free extract preparations of soluble enzymes from bacteria induced to express PEAMT had specific activity levels of 216.8 ± 41 nmol mg^{-1} protein min^{-1}. The presence of enzyme activity shows that the recombinant PEAMT enzyme obtained is functional. Recombinant PEAMT carries a polyhistidine-tag which allows for its purification using a cobalt metal affinity column. While this purification method significantly reduced the amount of contaminating proteins, it also caused a 13-fold reduction in PEAMT enzyme activity. The buffers and reagents used in the purification were not the reason for the loss of activity (see Results). One factor that has not yet been verified is a possible inhibition of PEAMT activity by the Co^{2+} column resin. Cobalt has been shown to be a potent inhibitor of PEAMT activity when this metal ion was added to enzyme assays (Smith *et al.*, 2000). When 10 mM $CoCl_2$ was added to the assay, PEAMT activity was inhibited 100%. Therefore, the interaction of PEAMT with the cation on this column is likely to have contributed to the loss of enzyme activity.

Using the recombinant PEAMT protein as antigen, polyclonal antibodies were generated that could detect as little as 10 ng native or 5 ng denatured PEAMT protein when diluted 1,000-fold. However, immunoblot analysis of crude spinach leaf extracts proved problematic due to the co-migration of PEAMT with the far more abundant LSU of Rubisco. This co-migration displaced PEAMT and caused the single band associated with PEAMT to be very diffuse. The subsequent detection of PEAMT protein by the antibody on the

developed Western blot showed a smudge where a single band for PEAMT was originally anticipated. This resolution problem was solved by immunoaffinity purification of PEAMT protein from crude leaf extracts using activated protein A agarose beads (see Materials and Methods). Western blot analysis of immuno-purified PEAMT yields a distinct band of 54 kDa, the Mr for PEAMT resolved electrophoretically under denaturing conditions reported by Smith *et al.* (2000). With a clearly resolved band, quantification of band intensity and size using the Kodak 1D Image Analysis Software could be used to compare the relative band intensities associated with the 54 kDa polypeptide in samples from leaves subjected to different treatments. Precise comparisons of treatment effect on PEAMT protein level would have been very difficult without the introduction of the immuno-purification strategy.

Responses to light and salinity

PEAMT activity, protein and transcript levels were examined in spinach plants exposed to various diurnal light/dark treatments. In spinach leaves, changes in the levels of PEAMT activity are positively correlated with changes in PEAMT protein levels under the treatments investigated: PEAMT specific activity and protein levels increase under conditions of continuous light to maximal levels after 24 h light and both activity and protein decrease in the dark to a low and constant level after 20 h of dark exposure (Fig. 9 and 11, respectively). Thus relative changes in the levels of PEAMT activity measured between extracts were shown to be accompanied by changes in PEAMT protein levels for those extracts as shown by immunoblot analysis. Smith *et al.* (2000) also showed a similar trend

with an indirect approach using photo affinity cross-linking of PEAMT protein to [^{3}H]-SAM. They report that PEAMT protein levels were likely highest in the presence of light and decreased to almost non-detectable levels in the dark. The authors acknowledged that the cross-linking strategy might lead to anomalous PEAMT protein level estimates if the SAM-binding site was somehow modified in plants exposed to the dark. Since it is highly unlikely that the polyclonal antibodies used in this study are specific towards a single site on PEAMT (and so their use to quantify PEAMT levels are not subject to the same concerns as the cross-linking approach), it is important to note that results obtained with both western blot hybridizations and UV-cross-linking studies lead to the same conclusions (Smith *et al.*, 2000; this work).

Changes in *peamt* transcript levels do not follow the same pattern of changes seen in protein or activity levels. In fact, *peamt* transcript levels cycle diurnally with maximal levels found during hours coinciding with a dark period and so during a time when PEAMT activity and protein are decreasing or virtually absent. Conversely, the lowest level of *peamt* transcripts are found during the hours associated with the normal light period, the time when both PEAMT activity and protein levels are increasing or at their peak.

Figure 9 shows that under conditions of continuous light, the same phase and amplitude of the rhythm in transcript level continues over at least two subjective light/dark cycles. In continuous darkness, transcript levels show a similar phase as the rhythm in continuous light during the first subjective light-dark cycle, but during the second subjective

dark period the amplitude is reduced and during the third subjective dark period the rhythm is suspended. Therefore, the oscillations in transcript levels diminish with prolonged exposure to darkness. The dampening of the circadian oscillation of transcript levels after transfer to continuous dark conditions is common (Pilgrim *et al.*, 1993; Millar and Kay,1991). In continuous darkness the dampening may be caused by a clock that no longer operates in continuous darkness or by the presence or absence of an additional, as yet unknown signal, that does not allow the circadian oscillation to be seen (Pilgrim *et al.*, 1993).

Circadian oscillations in PEAMT transcript abundance have not yet been reported. However, many genes involved in metabolic pathways exhibit circadian changes in their messenger RNA levels. Harmer *et al.* (2000) used microarray analysis of mRNA in plants subjected to 48 h of continuous light to show that 453 of the 8,200 different *Arabidopsis* genes represented on their array are circadian-regulated. Several of the genes on the array encode proteins of unknown function that were found to cycle in a circadian fashion (Harmer *et al.*, 2000). The *Arabidopsis peamt* sequence does not appear on the publicly available microarray data, but a related gene sequence (GenBank Accession AA394465, Clone ID 135E2XP) has 82% nucleotide identity with the *Arabidopsis peamt* sequence (found in the Stanford Microarray Database; http://daisy.stanford.edu/MicroArray/SMD/). Schaffer *et al.* (2001) shows the expression of this EST to be dark-induced according to the analysis of microarray data obtained for *Arabidopsis* plants under one normal light/dark cycle. It would be interesting to determine if genes related to PEAMT may be circadian-regulated and might

also display a similar circadian rhythm in transcript abundance as that seen for spinach *peamt* under continuous light.

While the *peamt* transcript is circadian-regulated, neither PEAMT activity nor protein levels display a comparable circadian pattern. Circadian rhythms are suggested to provide a means by which plants can fine-tune their metabolic activities in response to environmental changes thereby providing an adaptive advantage (Ouyang *et al.*, 1998). The biochemical basis for these rhythms are variable as are the times when peaks and troughs arise (Harmer *et al.*, 2000). Different rhythms for transcript levels of different genes may be caused by differential rates of transcription or from differential mRNA stability (Pilgrim *et al.*, 1993; McClung, 2000). In this study, transcript levels of *peamt* were shown to undergo circadian changes that peak during the dark period but the mechanism(s) underlying the circadian oscillations in transcript levels are unknown.

It may be that elevated *peamt* transcript levels in the dark may arise in anticipation of the onset of the light period and can facilitate a large and immediate increase in PEAMT protein and activity levels that need to be present in the light. There are a large number of genes whose products are involved in photosynthesis and are circadian-regulated to anticipate dawn and dusk (Harmer *et al.*, 2000). One group of enzymes catalysing reactions in the phenylpropanoid biosynthetic pathway are all circadian-regulated and peak during the subjective night (Harmer *et al.*, 2000). In this case, however, oscillations in transcript levels are parallelled by oscillations in protein abundance since these proteins are involved in the

photosynthetic machinery and are required as soon as the day begins (Somers *et al.*, 1999). It is likely that post-transcriptional regulatory mechanisms that may or may not be light-regulated lead PEAMT activity to be present in the light and low in the dark. These fine metabolic controls on PEAMT activity may be necessary given that the synthesis of one molecule of PCho from EA requires the equivalent of 7 ATP and so PCho, and hence choline or PtdCho production, is a pathway with a high energy requirement (Weretilnyk *et al.*, 2001).

PEAMT activity is also salt-regulated and so we investigated PEAMT transcript levels comparing control, unsalinized plants with plants salinized to 200 mM NaCl by harvesting tissue over a normal day and night. Salt-stressed spinach plants have been reported to increase in PEAMT activity and protein levels relative to control, unstressed plants during the light period and that these increases only take place in plants salt-stressed in the light (Smith *et al.*, 2000). This study shows that transcript levels associated with *peamt* in leaves of salinized plants are higher than those of control plants during a normal light-dark cycle and that the increase in transcripts is not brought about by suspension of the circadian rhythm associated with these transcript levels. Therefore, salinization increases the amplitude of the oscillation in PEAMT transcript but not the period or phase of the rhythm. In summary, changes in water availability and light influence PEAMT activity, protein and transcript levels but they are not likely regulated by controls that respond to the same stimuli. Promoters or post-transcriptional mechanisms must therefore be regulated by both a circadian clock and by other environmental factors influenced by salt treatment. An example of dual regulation of gene expression occurs

in genes encoding the chlorophyll a/b-binding proteins of photosystem II which are both circadian and light quality-regulated (Lemaire *et al.*, 1999).

Future avenues of investigation

PEAMT is the only enzyme in plants shown to catalyse the *N*-methylation of PEA to PMEA. However, the two subsequent *N*-methylations along the P-base route to produce PCho can be catalysed by both PEAMT and PMEAMT. These P-base *N*-methylating enzymes respond differently to different environmental stimuli (Weretilnyk *et al.*, 1995). When plants are salinized to 300 mM salt PEAMT activity increases 2-fold whereas PMEAMT activity and PDEAMT activities only increase by approximately 1.5-fold (Summers and Weretilnyk, 1993). Also PEAMT activity is light-regulated while PMEAMT and PDEAMT activities are apparently unaffected by light and dark (Weretilnyk *et al.*, 1995). The enzymes PEAMT and PMEAMT may, however, be structurally similar sharing, for example, amino acid sequences since they both catalyse the *N*-methylations of PMEA and PDEA. Therefore, using PEAMT as a template, Burian (2000) used the sequence of the *Arabidopsis* gene encoding PEAMT to identify three genes related to this sequence in the *Arabidopsis* genome data base (http://www.tigr.org/tdb/agi/index.html). If *Arabidopsis peamt* is also circadian-regulated, similarities and differences of these genes to that of the PEAMT sequence as well as the DNA sequence of regions up and down stream of each locus may reveal possible translational and post-transcriptional regulatory mechanisms. For example, using similar experimental design to this thesis, determinations of PMEAMT activity, protein and transcript levels could be

undertaken to determine whether circadian changes are present for transcript abundance despite the absence of such changes for PMEAMT activity. If *pmeamet* transcripts do not show circadian rhythms, a comparison with *peamt* may identify properties of the *peamt* transcript or factor(s) regulating expression of this gene needed for circadian changes.

Other enzymes involved in the *N*-methylation activities of PEAMT and PMEAMT, such as *S*-adenosylhomocysteine hydrolase (SAHH) or adenosine kinase (ADK) may also have circadian-regulated transcript abundance. The *N*-methylations catalysed by PEAMT and PMEAMT are dependent on SAM as a methyl donor and when the methyl groups are transferred from SAM, SAH is produced. Since SAH is a potent inhibitor of this reaction, SAH inhibition is prevented by its continuous removal through the combined actions of SAHH and ADK (Weretilnyk *et al.*, 2001). SAHH activity produces adenosine and homocysteine and adenosine is then converted to adenine mono- and diphosphate by ADK (Weretilnyk *et al.*, 2001). As for PEAMT, both SAHH and ADK activity levels are salt-regulated with incremental increases in activity with increasing salt stress. Therefore, it is possible that SAHH and ADK transcript levels are circadian-regulated and this should also be investigated.

Production of transgenic lines that constitutively overexpress PEAMT or contain no PEAMT expression would provide further information on nature of the mechanism(s) responsible for the circadian-regulation of *peamt* transcript levels. Studies with these plants may help identify mechanisms leading *peamt* transcript levels to show circadian behaviour and whether this gene and factors regulating its expression are conserved. The existence of

feedback loops, where PEAMT levels can influence *peamt* transcriptional or post-transcriptional regulation or the regulation of other proteins, may also be revealed. Discovery of post-transcriptional and post-translational mechanisms influencing PEAMT would make an important contribution towards our understanding of factors regulating PEAMT activity and how these factors might regulate PEAMT activity in transgenic plants engineered to overexpress this gene product.

APPENDIX 1a: Modification of *peamt* for subcloning into pET30a (+)

The DNA sequence of *peamt* cDNA modified to introduce *Nco* I and *Bam*H I restriction sites are highlighted in red and the oligonucleotide primers used to incorporated the changes by PCR are shown in blue. *Nco* I is created at the translation initiation site (**atg**) and *Bam*H I is ceated after the end of the longest open reading frame (**tga**). The *peamt* sequence shown is reported by Nuccio *et al.* (2000).

1 cattcatttg aagcgtggaa gtagtagttt tgtggtagag tgaatttgat actcctactg
61 ctcatgcggc agagaggcag ggcttcgaac cgtagatcca ggacttttc tcgttctcgc
121 attgccattg agggtcacta atacttttaa ctatctcctt ctttttcttt cccacaattt
181 ctgcgttttc acgcacatta atctcaccta ttttctagct tcttcatttt ctcaatcaat
241 ctctcgtgtt attatggccg cttcagctat gggagtgttg caagagagag aggtgttcaa
gtgttaccatggccg cttcag
301 gaaatactgg attgaacact ctgttgattt gactgttgag gctatgatgc ttgattcaca
361 agcttcagat cttgacaaag tggagcgacc tgaggtactt tccatgcttc caccttatga
421 aggaaagtct gtcttagaac tcggtgctgg tattggtcgt tttactggtg aattggccga
481 gaaagctagc caggtcatcg ctctggattt cattgagagt gttataaaga agaatgaaag
541 cataaatggg cattacaaaa atgtgaagtt tatgtgtgct gatgtgacat ctccaagtct
601 caacatttca ccaaattccg tggatatcat attctccaat tggctactca tgtatctttc
661 tgatgaagag gttgagcgtc tggttgaaag gatgttgaaa tggttgaagc caggaggata
721 cattttcttc agagaatctt gttttcatca atcaggagat cacaagcgca aaagcaatcc
781 aacccactac cgtgaaccta ggttctacac caagatcttc aaagaatgcc atatgcaaga
841 tgattctggg aactcctatg agctctccct aattggctgc aaatgtattg gagcttatgt
901 caaaagcaag aagaatcaga accagataag ctggttatgg cagaaagttg attcagagga
961 tgacaagggg ttccagcgat tcttggattc tagtcaatac aagtttaaca gcatactgcg
1021 ttatgagcgt gtatttggtc ctggttatgt tagtaccgga ggactcgaaa caaccaagga
1081 gtttgtatca aagcttgact tgaagcctgg ccagaaggtc ctagatgtgg gttgtggcat
1141 aggtggaggt gatttttaca tggcagagaa ctatgatgtt gaggttgttg gaattgatct
1201 ctccattaat atgatttctt ttgcccttga gcgctcaatt ggcctcaaat gtgctgttga
1261 gtttgaggtg gcagattgca ccaagaaaga ttaccctgaa aactcttttg atgtcatcta
1321 cagccgtgat accattctgc atattcagga caaacctgct ttatttagat ccttccacaa
1381 atggttgaaa cctggaggca aagttcttat tagtgactac tgtaagagtg ctggtacacc
1441 ttcagctgaa tttgctgcat acatcaggca gaggggatat gatctccacg atgtgaaggc
1501 atatggcaag atgcttaaag atgctggatt cgttgaggtt attgctgaga ataggactga
1561 ccagttcatt caagttctgc agaaggaact agatgctctt gaacaggaga aggatgactt
1621 cattgatgat ttctctgagg aggattataa cgacatagtt gatggttgga aggccaagtt
1681 ggtgaggact acagagggtg agcaacaatg gggtttgttc attgccaaga aaatgtgaag
1741 aatgagctgg tgaaagcagc acggtgcctt tttctagtat tagtttatca atgtattttc
gagctgg tgaaagcagg atcccg
1801 agttcatgga ctgtatatgc aaaatctacc aataagctgt gagttgcaaa ctgaaagatg
1861 atttcttata gtcacttctg aattagcaca agcagtgaag ttcgcataag aaactgaagg
1921 gaactcatgg agttgcagac gaaatcatca aaacggcaga acccactctc tatatagaga
1981 tctagtggtt aagttatgtg ttttgtacat tttccgttcc aagttcactc aatcttacca
2041 tcataatatc accgctttta cttctttata tggtggattg aagtcgaaac tctttgttag
2101 taatgtgtat tagtttgttg aaagtggaac ttgcaacaca cttattcaca agtgtgtagg
2161 gaaatatgga ttttgtatta gtatgtactg cacttagttg ttaaaaggat acttcctacg
2221 ttttcttctg ttgcaaaaaa aaaaaaaaaa aa

APPENDIX 1b: Genetic map of recombinant pET30a (+)

This circular DNA map of pET30a (+) vector shows the important features used in this work. The pET30a (+) vector contains a T7 cloning/expression region beginning with the T7 promoter and ending with the T7 terminator. Within this region are multiple cloning sites, only four restriction sites are shown on this map for simplicity. Insertion of the modified *peamt* sequence into the pET30a (+) vector was performed after both *peamt* and the vector were cut at the two restriction sites *Nco* I and *Bam*H I. The pET30a (+) vector also carries an N-terminal histidine-tag coding sequence within the T7 cloning/expression region. The gene encoding kanamycin resistance (neomycin phosphotransferase, *Npt* II) allows isolation of bacteria transformed with the plasmid by growth on media containing the antibiotic kanamycin.

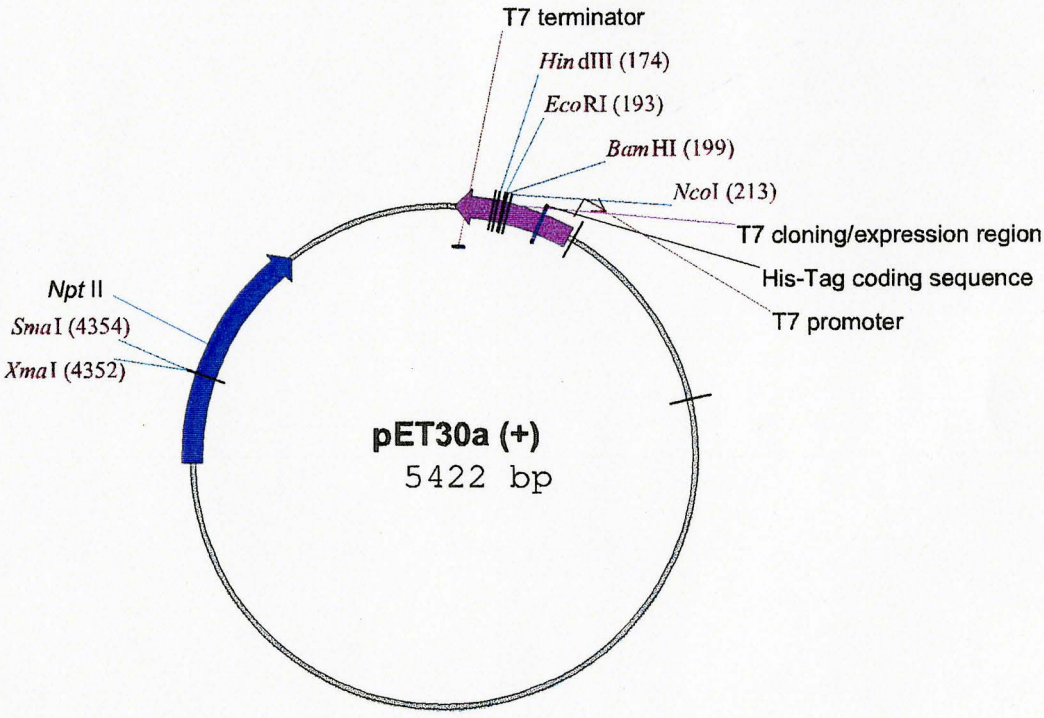
T7 terminator
Hin dIII (174)
EcoRI (193)
BamHI (199)
NcoI (213)
T7 cloning/expression region
His-Tag coding sequence
T7 promoter
Npt II
SmaI (4354)
XmaI (4352)
pET30a (+)
5422 bp

Appendix 1c: Sequence analysis of *peamt*

The sequencing results prepared by the Central DNA Facility, McMaster University where compared with the *Spinacia oleracea* PEAMT encoding sequence. The sequencing results show that the *peamt* insert was modified at the transcription initiation site to include the restriction site *Nco* I (bold, Panel A). Also the *peamt* insert was modified at the end of the longest open reading frame to include the restriction site *Bam*H I (bold, Panel B).

A


* translational initiation start site
Sequence results ACAAGG CCATGG CCGCTT CAGCTA TGGGAG.sequence continues
PEAMT GTGTTA TTATGG CCGCTT CAGCTA TGGGAG.sequence continues

B

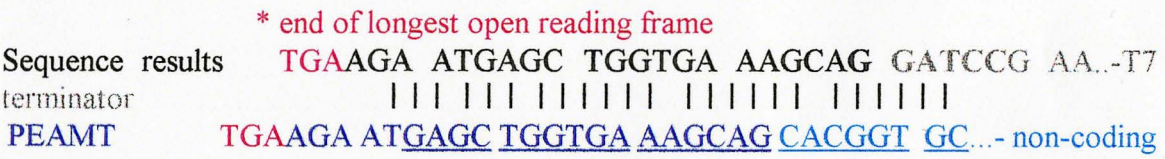
* end of longest open reading frame
Sequence results TGAAGA ATGAGC TGGTGA AAGCAG GATCCG AA..-T7
terminator
PEAMT TGAAGA ATGAGC TGGTGA AAGCAG CACGGT GC...- non-coding

APPENDIX 2: Verification of the covalent coupling of protein A agarose beads to antibodies raised to PEAMT

After the initial incubation of beads with antibody, the mixture is centrifuged and the supernatant is removed and retained. 'Pre-coupling' and 'post-coupling' samples of beads are also retained during the coupling procedure (see Materials and Methods). These bead samples along with 30 μL of the supernatant are mixed with 30 μL SDS solubilizing buffer and heated to 90 °C for 3 min and centrifuged. The solution above the 'Pre and Post-coupling' beads as well as an aliquot of SDS-denatured supernatant retained after the initial coupling of antibody to the beads was loaded onto a 7.5-15 % SDS-PAGE gradient gel. The arrow denotes the band corresponding to the immunoglobulin protein released from the beads by the SDS denaturation seen in the 'pre-coupling' lane. No comparable band is seen in the post-coupling lane, an indication that the coupling is successful.

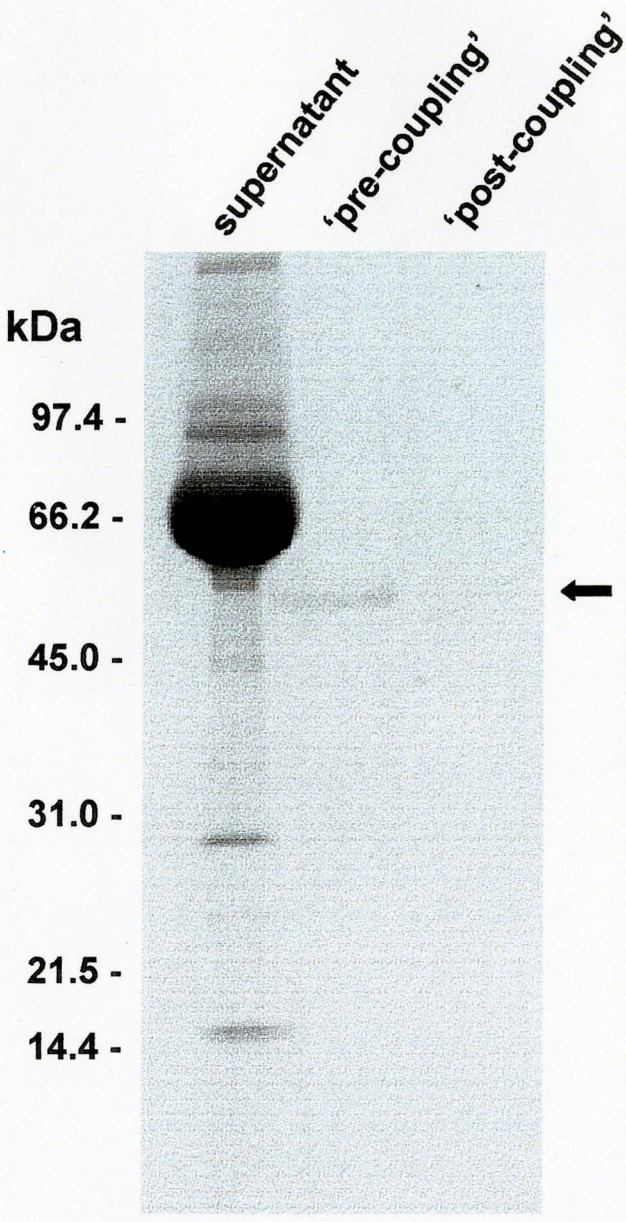
supernatant
'pre-coupling'
'post-coupling'
kDa
97.4 -
66.2 -
45.0 -
31.0 -
21.5 -
14.4 -

APPENDIX 3a: Quantification of total RNA

Representative wavelength scan of total RNA isolated from spinach leaves

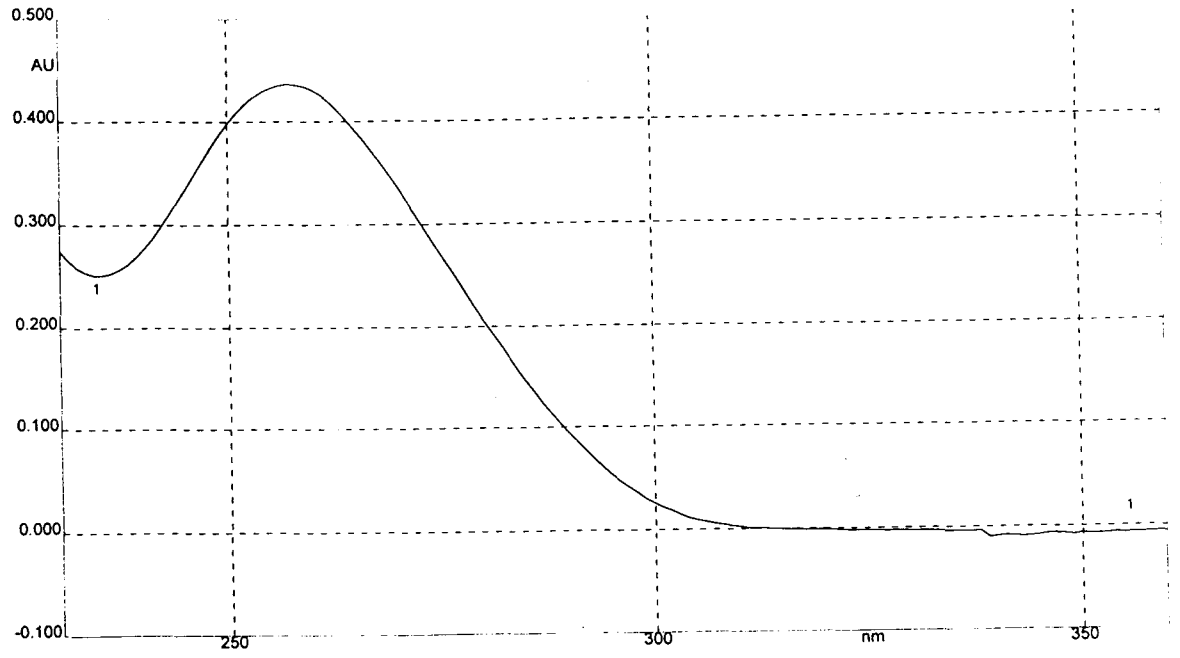

Quantification of a representative total RNA sample isolated from spinach leaves

OD_{310} = 0.0090
OD_{280} = 0.0989
OD_{260} = 0.1984

ratio OD_{260}/OD_{280} = 2.00

$\mu g\ mL^{-1} = OD_{260}\ (40\ \mu g\ mL^{-1} / OD_{260})$
$= 0.1984 \times 40\ \mu g\ mL^{-1} \times 160$ dilution
$= 1269.76$

APPENDIX 3b: Yield and quality of isolated total RNA

Total RNA isolated from plants exposed to continuous light

Time (h)	OD_{260}/OD_{280}	Total RNA concentration $\mu g\ mL^{-1}$
-12	1.89	6769.9
-8	1.80	8597.76
-4	2.06	3381.12
0	2.1	3824.64
4	2.2	3130.88
8	1.93	6202.88
12	2.1	2319.36
16	2.2	2931.2
20	2.0	6471.04
24	2.11	5013.76
28	2.21	2862.72
32	2.16	2188.8
36	1.88	10383.36
40	2.0	5117.44
44	2.14	3143.68
48	2.16	1648.64
52	1.87	6465.28
56	1.99	3213.44
60	1.89	1959.04

Total RNA isolated from plants exposed to continuous dark

Time (h)	OD_{260}/OD_{280}	Total RNA concentration $\mu g\ mL^{-1}$
0	1.99	3674.24
0.5	2.16	2608.28
1	2.28	2721.92
2	2.27	1465.6
3	2.19	1862.4
4	2.15	2401.92
5	2.13	3699.84
6	2.18	3846.4
12	2.19	2087.68
16	1.83	13454.08
20	1.84	5246.72
24	1.79	6800.0
28	1.8	5171.84
32	1.81	6656.64
36	1.81	7657.6
40	2.14	9244.8
44	1.88	11409.28
48	2.12	6701.44
52	1.95	9594.88
56	2.2	6800.64
60	2.13	10297.6

Total RNA isolated from unstressed plants under a normal light/dark cycle

Time (h)	OD_{260}/OD_{280}	Total RNA concentration $\mu g\ mL^{-1}$
0	2.2	6830.72
4	2.17	8007.68
8	2.22	7920.64
12	1.94	12823.04
16	1.83	10984.96

Total RNA isolated from salt-stressed plants under a normal light/dark cycle

Time (h)	OD_{260}/OD_{280}	Total RNA concentration $\mu g\ mL^{-1}$
0	2.26	5091.84
4	2.25	5122.56
8	2.22	7453.44
12	2.04	5873.93
16	2.08	6458.88

LITERATURE CITED

Apse MP, Aharon GS, Snedden WA, Blumwald E (1999) Salt tolerance conferred by over-expression of a vacuolar Na^+/H^+ antiport in *Arabidopsis*. Science 285: 1256-1258

Arakawa E, Takabe T, Sugiyama T, Akazawa T (1987) Purification of betaine-aldehyde dehydrogenase from spinach leaves and preparation of its antibody. J Biochem 101: 1485-1488

Bewley JD (1979) Physiological aspects of desiccation tolerance. Annu Rev Plant Physiol 30:195-205

Boyer, JT (1982) Plant productivity and the environment. Science 218: 443-448.

Bradford MM (1976) A rapid and sensitive method for the quantitation of microgram quantities of protein utilizing the principle of protein-dye binding. Anal Biochem 72: 248-329

Bray E A, Bailey-Serres J, Weretilnyk E (2000) Responses to abiotic stresses. *In* B Buchanan, W Gruissem, R Jones, eds, Biochemistry and molecular biology of plants. Amer Soc Plant Physiol, Rockville, Maryland. 1367 pp

Brouquisse R, Weigel P, Rhodes D, Yocum CF, Hanson AD (1989) Evidence for a ferredoxin-dependent choline monooxygenase from spinach chloroplast stroma. Plant Physiol 90: 322-329

Burian TZ (2000) Purification and properties of *S*-adenosyl-L-methionine: phophomethylethanolamine *N*-methyltransferase from spinach. M.Sc. Thesis. McMaster University

Burnet M, Lafontaine PJ, Hanson AD (1995) Assay, purification, and partial characterization of choline monooxygenase from spinach. Plant Physiol 108: 581-588

Datko AH, Mudd SH (1988) Phosphatidylcholine synthesis: differing patterns in soybean and carrot. Plant Physiol 88: 854-961

Davies WJ, Mansfield TA, Hetherington AM (1990) Sensing of soil water status and the regulation of plant growth and development. Plant Cell Env 13: 709-719

Dunlap JC (1999) Molecular basis for circadian clocks. Cell 96: 271-290

Eloranta TO, Kajander EO, Raina AM (1976) A new method for the assay of tissue *S*-adenosylhomocysteine and *S*-adenosylmethionine. Biochem J 160: 287-294

Engelmann W, Johnsson A (1998) Rhythms in organ movement. *In* PJ Lumsden, AJ Millar, eds, Biological rhythms and photoperiodism in plants. BIOS Scientific Publishers, Oxford, pp 99-118

Epstein E, Rains DW (1987) Advances in salt tolerance. Plant Soil 99: 17-29

Finlayson SA, Lee I, Mullet JE, Morgan PW (1999) The mechanism of rhythmic ethylene production in sorghum. The role of phytochrome B and simulated shading. Plant Physiol 119: 1083-1089

Grumet R, Hanson AD (1986) Genetic evidence for an osmoregulatory function of glycine

betaine accumulation in barley. Aust. J. Plant Physiol 13: 353-364

Guy RD, Warne PG, Reid DM (1984) Glycinebetaine content of halophytes: Improved analysis by liquid chromatography and interpretations of results. Physiol Plant 61: 195-202

Hanson AD, Hitz WD (1982) Metabolic responses of mesophytes to plant water deficits. Annu. Rev. Plant Physiol 73: 834-843

Hanson AD, May AM, Grument R, Bode J, Jamieson GC, Rhodes D (1985) Betaine synthesis in chenopods: localization in chloroplasts. Proc Natl Acad Sci USA 82: 3678-3682

Hanson AD, Rathinasabapathi B, Chamberlain B, Gage DA, (1991) Comparative physiological evidence that β-alanine betaine and choline-*O*-sulfate act as compatible osmolytes in halophytic *Limonium* species. Plant Physiol 97: 1199-1205

Hanson AD, Rhodes D (1983) ^{14}C Tracer evidence for synthesis of choline and betaine via phosphoryl base intermediates in salinized sugar beet leaves. Plant Physiol 71:692-700

Hanson AD, Scott NA (1980) Betaine synthesis from radioactive precursors in attached, water stressed barley leaves. Plant Physiol 66:342-348

Hanson AD, Wyse R (1982) Biosynthesis, translocation, and accumulation of betaine in sugar beet and its progenitors in relation to salinity. Plant Physiol 70: 1191-1198

Harlow E, Lane D (1988) Antibodies: a laboratory manual. Cold Spring Harbor Laboratory Press, Cold Spring Harbor, New York. 726 pp

Harmer SL, Hogenesch JB, Straume M, Chang H, Han B, Zhu T, Wang X, Kreps JA, Kay

SA (2000) Orchestrated transcription of key pathways in *Arabidopsis* by the circadian clock. Science 290: 2110-2113

Hartwell J, Smith LH, Wilkins MB, Jenkins GI, Nimmo HG (1996) Higher plant phosphoenolpyruvate carboxylase kinase is regulated at the level of translatable mRNA in response to light or a circadian rhythm. Plant J 10: 1071-1078

Hasegawa PM, Bressan RA, Zhu J, Bohnert HJ (2000) Plant cellular and molecular responses to high salinity. Annu Rev Plant Physiol Plant Mol Biol **51**: 463-499

Hayashi AH, Mustardy L, Deshnium P, Ida M, Murata N (1997) Transformation of *Arabidopsis thaliana* with the codA gene for choline oxidase; accumulation of glycine betaine and enhanced tolerance to salt and cold stress. Plant J 12: 133-142

Heintzen C, Nater M, Apel K, Staiger D (1997) *At*GRP7, a nuclear RNA-binding protein as a component of a circadian-regulated negative feedback loop in *Arabidopsis thaliana*. Proc Natl Acad Sci USA 94: 8515-8520

Hennessey TL, Field CB (1991) Circadian rhythms in photosynthesis: Oscillations in carbon assimilation and stomatal conductance under constant conditions. Plant Physiol 96: 831-836

Hennessey TL, Field CB (1992) Evidence of multiple circadian oscillators in bean plants. J Biol Rhythms 7: 105-113

Hitz WD, Rhodes D, Hanson AD (1981) Radiotracer evidence implicating phosphoryl and phophatidyl bases as intermediates in betaine synthesis by water stressed barley leaves.

Plant Physiol 68: 814-822

Hoagland DR, Arnon DI (1950) The water-culture method for growing plants without soil. Univ California Berkeley Coll Agr Circ 347:1-32

Johnson CH, Knight M, Trewavas A, Kondo T (1998) A clock-work green: circadian programs in photosynthetic organisms. *In* PJ Lumsden, AJ Millar, eds, Biological rhythms and photoperiodism in plants. BIOS Scientific Publishers, Oxford, pp 1-34

Jolivet Y, Hamelin J, Larher F (1983) Osmoregulation in halophytic higher plants: the protective effects of glycine betaine and other related solutes against the oxalate destabilisation of membranes in beet root cells. Z Pflanzenphysiol 109: 171-180

Jones TL, Tucker DE, Ort DR (1998) Chilling delays circadian pattern of sucrose phosphate synthase and nitrate reductase activity in tomato. Plant Physiol 118: 149-158

Jones TL, Ort DR (1997) Circadian regulation of sucrose phosphate synthase activity in tomato by protein phosphatase activity. Plant Physiol 113: 1167-1175

Kolar C, Ádám É, Schäfer E, Nagy F (1995) Expression of tobacco genes for light-harvesting chlorophyll a/b binding proteins of photosystem II is controlled by two circadian oscillators in a developmentally regulated fashion. Proc Natl Acad Sci USA 92: 2174-2178

Kondo T, Tsinoremas NF, Golden SS, Johnson CH, Kutsuna S, Ishiura M (1994) Circadian clock mutants of cyanobacteria. Science 266: 1233-1236

Koshland DE (1984) Control of enzyme activity and metabolic pathways. Trends Biochem

Sci 9: 155-159

Kramer PJ (1983) Problems in water relations of plants and cells. Intl Rev Cyt 85: 253-291

Kreps JA, Simon AE (1997) Environmental and genetic effects on circadian clock -regulated gene expression in Arabidopsis. Plant Cell 9: 297-304

Lemaire SD, Stein M, Issakidis-Bourguet E, Keryer E, Benoit V, Pineau B, Gérard-Hirne C, Miginiac-Maslow M, Jacquot J (1999) The complex regulation of ferredoxin/thioredoxin-related genes by light and the circadian clock. Planta 209: 221-229

Lorenzin D, Webb C, Summers PS, Weretilnyk EA (2001) Enzymes of choline synthesis in diverse plants: variation in phosphobase *N*-methyltransferase activities. Can J Bot 79: 897-904

Maniatis T, Fritsch E, Sambrook J (1982) Molecular cloning: A laboratory manual. Cold Spring Harbor Laboratory Press, Cold Spring Harbor, New York.

McClung CR (2000) Circadian rhythms in plants: a millennial view. Physiol Plant 109: 359-371

McClung CR (2001) Circadian rhythms in plants. Annu Rev Plant Physiol Plant Mol Biol 52: 139-162

McCree KJ (1986) Whole-plant carbon balance during osmotic adjustment to drought and salinity stress Aust J Plant Physiol 13: 33-43

McCue KF, Hanson AD (1990) Drought and salt tolerance: towards understanding and

application. Trends Biotech 8: 358-362.

McDonnell E, Wyn Jones RG (1988) Glycinebetaine biosynthesis and accumulation in unstressed and salt-stressed wheat. J Exp Bot 39: 421-430

McNeil SD, Nuccio ML, Hanson AD (1999) Betaines and related osmoprotectants. Targets for metabolic engineering of stress resistance. Plant Physiol 120: 945-949

McNeil SD, Nuccio ML, Rhodes D, Shackar-Hill, Y, Hanson, AD (2000) Radiotracer and computer modelling evidence that phospho-base methylation is the main route of choline synthesis in tobacco. Plant Physiol 123: 371-380

McNeil SD, Nuccio ML, Ziemak MJ, Hanson AD (2001) Enhanced synthesis of choline and glycine betaine in transgenic tobacco plants that overexpress phosphoethanolamine *N*-methyltransferase. Proc Natl Acad Sci USA 98:10001-10005

Merrow MW, Garceau NY, Dunlap JC (1997) Dissection of a circadian oscillation into discrete domains. Proc Natl Acad Sci USA 94: 3877-3882

Millar AJ, Carré IA, Strayer CA, Chua N, Kay SA (1995) Circadian clock mutants in *Arabidopsis* identified by luciferase imaging. Science 267: 1161-1163

Millar AJ, Kay SA (1991) Circadian control of *cab* gene transcription and mRNA accumulation in *Arabidopsis*. Plant Cell 3: 541-550

Morgan JM (1986) The effects of N nutrition on the water relations and gas exchange characteristics of wheat (*Triticum aestivum* L.). Plant Physiol 80: 52-58

Morse D, Hastings JW, Roenneberg T (1994) Different phase responses of the two circadian

oscillators in *Gonyaulax*. J Biol Rhythms 9: 263-274

Mudd SH, Datko AH (1986) Methionine methyl group metabolism in *Lemna*. Plant Physiol 81: 103-114

Mudd SH, Datko AH (1989a) Synthesis of ethanolamine and its regulation in *Lemna paucicostata*. Plant Physiol 91:587-597

Mudd SH, Datko AH (1989b) Synthesis of methylated ethanolamine moieties. Regulation by choline in soybean and carrot. Plant Physiol 90: 306-310

Mudd SH, Datko AH (1989c) Synthesis of methylated ethanolamine moieties. Regulation of choline in *Lemna*. Plant Physiol 90: 296-305

Müller H, Eckert, H (1989) Simultaneous determination of monoethanolamine and glycine betaine in plants. J Chromat 479: 452-458.

Nagy F, Fejes E, Wehmeyer B, Dallman G, Schafer E (1993) The circadian oscillator is regulated by a very low fluence response of phytochrome in wheat. Proc Natl Acad Sci USA 90: 6290-6294

Nelville DM (1971) Molecular weight determination of protein-dodecylsulphate complexes by gel electrophoresis in a discontinuous buffer system. J Biol Chem 246: 6328-6334

Nilsen ET, Orcutt DM (1996) The physiology of plants under stress. John Wiley and Sons, Inc., New York. pp 304-343

Nuccio ML, Rhodes D, McNeil SD, Hanson AD (1999) Metabolic engineering of plants for osmotic stress resistance. Curr Opin Plant Biol 2:128-134

Nuccio ML, Russell BL, Nolte KD, Rathinasabapathi B, Gage DA, Hanson AD (1998) The endogenous choline supply limits glycine betaine synthesis in transgenic tobacco expressing choline monooxygenase. Plant J 16: 487-496

Nuccio ML, Ziemak MJ, Henry SA, Weretilnyk EA, Hanson AD (2000) cDNA cloning of phosphoethanolamine *N*-methyltransferase from spinach by complementation in *Schizosaccharomyces pombe* and characterization of the recombinant enzyme. J Biol Chem 275: 14095-14101

Ouyang Y, Andersson CR, Kondo T, Golden SS, Johnson CH (1998) Resonating circadian clocks enhance fitness in cyanobacteria. Proc Natl Acad Sci USA 95: 8660-8664

Pan S, Moreau RA, Yu C, Huang AHC (1981) Betaine accumulation and betaine-aldehyde dehydrogenase in spinach leaves. Plant Physiol 67: 1105-1108

Pasternak, D. (1987) Salt tolerance and crop production - a comprehensive approach. Annu Rev Phytopathol 25: 271-291

Pilgrim ML, Caspar T, Quail PH, McClung CR (1993) Circadian and light-regulated expression of nitrate reductase in *Arabidopsis*. Plant Mol Biol 23: 349-364

Prud'homme M, Moore TS (1992) Phosphatidylcholine synthesis in castor bean endosperm. Plant Physiol 100: 1527-1535

Raven PH, Evert RF, Eichhorn SE (1999) Biology of Plants 6th edition. W.H. Freeman and Company, New York.

Rhodes D (1987) Metabolic Responses to Stress. *In* DD Davis, eds, The Biochemistry of

Plants, Vol 12, Academic Press, Inc. New York. pp 201-241

Rhodes D, Hanson AD (1993) Quaternary ammonium and tertiary sulfonium compounds in higher plants. Annu Rev Plant Physiol Plant Mol Biol 44: 357-384

Robinson SP, Jones GP (1986) Accumulation of glycine betaine in chloroplasts provides osmotic adjustment during salt stress. Aust J Plant Physiol 13:659-668.

Roenneberg T, Morse D (1993) Two circadian oscillators in one cell. Nature 362: 362-364

Russel BL, Rathinasabapathi B, Hanson AD (1998) Osmotic stress induces expression of choline monooxygenase in sugar beet and amaranth. Plant Physiol 116: 859-865

Sambrook J, Fritsch EF, Maniatis T (1989) Molecular cloning: A laboratory manual 2nd edition. Cold Spring Harbor Laboratory Press, Cold Spring Harbor, New York.

Schaffer R, Landgraf J, Accerbi M, Simon V, Larson M, Wisman E (2001) Microarray analysis of diurnal and circadian-regulated genes in *Arabidopsis*. Plant Cell 13: 113-123

Smith DD, Summers PS, Weretilnyk EA (2000) Phosphocholine synthesis in spinach: Characterization of phosphoethanolamine *N*-methyltransferase. Physiol Plant 108: 286-294

Somers DE (1999) The physiology and molecular basis of the plant circadian clock. Plant Physiol 121: 9-19

Somers D, Devlin P, Kay SA (1998) Phytochromes and cryptochromes in the entrainment of the *Arabidopsis* circadian clock. Science 282: 488-490

Storey R, Wyn Jones RG (1975) Betaine and choline levels in plants and their relationship to NaCl stress. Plant Sci Lett 4: 161-168.

Storey R, Wyn Jones RG (1977) Quaternary ammonium compounds in plants in relation to salt resistance. Phytochemistry 16: 447-453.

Summers PS, Weretilnyk EA (1993) Choline synthesis in spinach in relation to salt stress. Plant Physiol 103: 1269-1276

Taiz L, Zeiger E (1998) Plant Physiology 2nd ed., Sinauer Associates, Inc., Sunderland, Massachusetts, 944 pp

Thain SC, Hall A, Millar AJ (2000) Functional independence of multiple circadian clocks that regulate plant gene expression. Curr Biol 10: 951-956

Trossat C, Rathinasabapathi B, Hanson AD (1997) Transgenically expressed betaine aldehyde dehydrogenase efficiently catalyses oxidation of dimethylsulfoniopropionaldehyde and ω aminoaldehydes. Plant Physiol 113: 1457-1461

Wallevick K, Jensenius JC (1982) A simple and reliable method for drying of polyacrylamide slab gels. J Biochem Biophys Methods 6: 17-21

Weigel P, Lerma C, Hanson AD (1988) Choline oxidation by intact spinach chloroplasts. Plant Physiol. **86**: 0054-0060

Weigel P, Weretilnyk EA, Hanson AD (1986) Betaine aldehyde oxidation by spinach chloroplasts. Plant Physiol 82: 753-759

Weretilnyk EA, Alexander KJ, Drebenstedt M, Snider JD, Summers PS, Moffatt BA (2001)

Maintaining methylation activities during salt stress. The involvement of adenosine kinase. Plant Physiol 125: 856-865

Weretilnyk EA, Hanson, AD (1988) Betaine aldehyde dehydrogenase polymophism in spinach: genetic and biochemical characterization. Biochem Genet 26: 143-151

Weretilnyk EA, Hanson AD (1989) Betaine aldehyde dehydrogenase from spinach leaves: purification, *in vitro* translation of the mRNA and regulation by salinity. Arch Biochem Biophys 271: 56-63

Weretilnyk EA, Hanson AD (1990) Molecular cloning of a plant betaine-aldehyde dehydrogenase, an enzyme implicated in adaptation to salinity and drought. Proc Natl Acad Sci USA 87: 2745-2749

Weretilnyk EA, Summers PS, (1992) Betaine and choline metabolism in higher plants. *In* BK Singh, HE Flores, JC Shannon, eds, Biosynthesis and molecular regulation of amino acids in plants. Amer Soc Plant Physiol, Rockville, MD, pp 89-97

Weretilnyk EA, Smith DD, Wilch GA, Summers PS (1995) Enzymes of choline synthesis in spinach: response of phospho-base *N*-methyltransferase activities to light and salinity. Plant Physiol 109:1085-1091

Wilkins MB (1992) Circadian rhythms: their origin and control. New Phytol 121: 347-375

Wray W, Boulikas T, Wray VP, Hancock R (1982) Silver staining of proteins in polyacrylamide gels. Anal Biochem 118: 197-203

Wyn Jones RG, Gorham J (1983) Osmoregulation. *In* CB Osmond, JH Ziegler, eds,

Encyclopedia of plant physiology, New Series Vol 12 C, Springer-Verlag; New York, pp 35-58

Wyn Jones RG, Storey R (1981) Betaines. *In* LG Paleg, D Aspinall, eds, Physiology and biochemistry of drought resistance in plants. Academic Press, Australia, pp 171-204

Yeo AR (1998) Molecular biology of salt tolerance in the context of whole-plant physiology. J Exp Bot 49: 915-929

Yeo AR, Caporn SJM, Flowers TJ (1985) The effect of salinity upon photosynthesis in rice (*Oryza sativa* L.): Gas exchange by individual leaves in relation to their salt content. J Exp Bot 36:1240-1248